REVIEWS OF MODERN PHYSICS VOLUME 21, NUMBER 4 OCTOBER, 1949

Interaction of Shock Waves*

WALKER BLEAKNEY
Palmer Physical Laboratory, Princeton University, Princeton, New Jersey

AND

A. H. TAUB
Department of Mathematics, University of Illinois, Urbana, Illinois

I. INTRODUCTION

1. Shock Waves

WHEN disturbances of finite amplitude are propagated in perfect fluids or gases, that is, those with no viscosity or heat conductivity, discontinuities in pressure and velocity of the medium may occur. These are called shock waves or shocks. The reason for their development may be readily seen in the case of one-dimensional flow such as occurs in a tube of uniform cross section when a disturbance caused by the motion of a piston at one end is propagated down the tube.

The velocity u of the piston at any time is communicated to the gas and propagates down the gas with the velocity of sound c relative to the gas.[a] Hence, relative to the tube, the velocity u is propagated with the speed $c+u$ in the direction away from the piston. Now if the piston moves to compress the gas in the tube, that is, to decrease the volume of the gas, then the velocity of sound increases since the temperature and density increase. Thus, the greater the velocity the greater the speed with which it is propagated. If this process continued indefinitely, lesser velocities would be overtaken by greater ones and we would have two values of the velocity at a given place in the gas which is impossible.

However, before this occurs, there will be a time at which the velocity profile of the gas, that is, the velocity *versus* distance curve, has a vertical shape. In this case, the differential equations governing the motion break down and the basis for the statement that the fluid velocity u is propagated with the velocity $c+u$, is no longer true. However, the laws of conservation of mass, momentum, and energy may be applied to give a description of the behavior of such discontinuities.

Before formulating these laws for a perfect fluid it may be pertinent to point out that it is a consequence of the non-linear character of the equations governing the propagation of finite disturbances that is in part responsible for the prediction of the formation of the discontinuities. Thus, in the example mentioned above, it is essential to the argument that the local velocity of sound c be greater at points where the velocity of the gas is large than where it is small. This is the case for a compressive motion of the piston because the disturbances which have passed over the gas have changed its character (heated it) and hence subsequent disturbances are traveling in a different medium than the original ones. This taking into account of the change in the medium produced by one part of the phenomenon in the discussion of a subsequent part is accomplished mathematically by the non-linear terms in the equations of motion.

The non-linear character alone is not enough to cause discontinuities for if, in the example given above, the piston motion were such as to increase the volume of the gas in the tube, that is, if a rarefaction wave were propagated down the tube, then the local velocity of sound would decrease with increasing fluid velocity and even if a discontinuity were originally present it would disappear with time. The fact that only compression shocks are found in media which behave approximately like ideal gases is in agreement with the second law of thermodynamics as will be seen later.

In the above discussion we have neglected the effects of heat conductivity and viscosity which may be expected to be of importance where large gradients in temperature and velocity develop. We shall see that taking these into account has the effect of smoothing out the discontinuities, thus giving the shock wave a structure as contrasted to a mathematical discontinuity. However, this structure is confined to a very small region and away from this region the theory of a perfect fluid is a good approximation.

2. Conservation Equations

The differential equations of hydrodynamics are the mathematical formulation of the laws of conservation of mass momentum and energy. We shall first state these laws in integral form and thus obtain the equations governing the motion irrespective of the existence of discontinuities.

Let ξ^i $(i=1, 2, 3)$ be the Cartesian coordinates (relative to a fixed coordinate system) of a particle in the fluid at some time t_0, and let x^i be the Cartesian coordinates of the same point at some later time t. The ξ^i are the so-called Lagrange coordinates and the x^i the Euler ones. The path described "by the particle ξ^i" is then given by

$$x^i=x^i(\xi^i, t). \tag{2.1}$$

* This work was supported in part by the ONR N6ori-105, Task Order II.
[a] See Appendix D for a collected list of symbols.

This curve is also called the stream line of the particle ξ^i. The velocity of any particle of the fluid is given by

$$u^i = dx^i/dt,$$

where the ξ^i are kept constant. In general, any function of the x's and t may be regarded as a function of the ξ's and t and conversely. We shall denote partial differentiation with respect to t for fixed ξ by the symbol d/dt and partial differentiation with respect to t with fixed x^i by $\partial/\partial t$. Thus, in general we will have

$$\frac{df}{dt} = \frac{\partial f}{\partial t} + \frac{dx^i}{dt}\frac{\partial f}{\partial x^i} = \frac{\partial f}{\partial t} + u^i \frac{\partial f}{\partial x^i},$$

where we have used the convention that a repeated index is summed unless otherwise noted.

Let $V(t)$ be the volume occupied at time t by the fluid originally in the volume V_0 enclosed by the surface S_0, and let $S(t)$ be the surface enclosing $V(t)$ and hence that surface which contains the particle originally in S_0. We shall want to consider integrals of the form

$$I(t) = \int_{V(t)} f(x^i, t) dV \tag{2.2}$$

and their time derivatives. We note that

$$I(t) = \int_{V_0} f(x(\xi, t), t) J dV_0, \tag{2.3}$$

where J is the Jacobian of the transformation $\xi^i \rightarrow x^i$ given by (2.1). That is,

$$J = \det(\partial x^i / \partial \xi^j), \tag{2.4}$$

and from the law for differentiating a determinant we have

$$\frac{dJ}{dt} = J \frac{\partial u^i}{\partial \xi^j}\frac{\partial \xi^j}{\partial x^i} = J \frac{\partial u^i}{\partial x^i}. \tag{2.5}$$

It follows directly from (2.2) or by use of (2.3) to (2.5) that if f has continuous derivatives with respect to x, y, z, and t throughout the volume $V(t)$, then

$$\frac{dI}{dt} = \int_{V(t)} \frac{\partial f}{\partial t} dV + \int_{S(t)} f u^i \lambda_i dS = \int_{V(t)} \left(\frac{\partial f}{\partial t} + \frac{\partial (f u^i)}{\partial x^i} \right) dV, \tag{2.6}$$

where λ_i is the normal to the surface $S(t)$ drawn away from the volume of integration. The quantity $u^i \lambda_i$ is the velocity of the fluid normal to the surface $S(t)$.

If there exists a surface $\Sigma(t)$ inside $V(t)$, which for simplicity we assume divides $V(t)$ into two parts $V_1(t)$ and $V_2(t)$ such that f is discontinuous across Σ but has continuous derivatives in $V_1(t)$ and $V_2(t)$, then we may write

$$I(t) = \int_{V_1(t)} f dV + \int_{V_2(t)} f dV = \int_{V_1 + V_2} f dV. \tag{2.7}$$

The bounding surface S of V will be divided into two parts by the curve of intersection of the surface Σ with S. We shall denote the parts of S which partially bound V_1 and V_2, respectively, by S_1 and S_2. Then

$$\frac{dI}{dt} = \int_{V_1 + V_2} \frac{\partial f}{dt} dV + \int_{S_1 + S_2} f u^i \lambda_i dS + \int_{\Sigma} [f] V_n d\Sigma, \tag{2.8}$$

where

$$[f] = f_1 - f_2, \tag{2.9}$$

that is, $[f]$ is the difference of the values of f on the V_1 and V_2 sides of Σ and V_n is the component of the velocity of Σ in the direction of the normal to Σ drawn from V_1 to V_2.

If the function f in Eq. (2.4) is identified with $\rho(x, t)$, the density of the gas, then

$$M = \int_{V(t)} \rho dV$$

is the mass of the gas contained in the volume $V(t)$. The law of conservation of mass is the statement that

$$dM/dt = 0$$

for arbitrary volumes $V(t)$. Thus, in regions of continuous flow we must have (see Eq. (2.6))

$$\frac{\partial \rho}{\partial t} + \frac{\partial (\rho u^i)}{\partial x^i} = \frac{d\rho}{dt} + \rho \frac{\partial u^i}{\partial x^i} = 0. \tag{I}$$

Incidentally, we may note that a first integral of this equation may readily be obtained. If $\rho_0(\xi)$ is the density of the fluid at time t_0 then from (2.3) it follows that

$$\int_{V_0} \rho J dV_0 = \int_{V_0} \rho_0 dV_0$$

for arbitrary volumes V_0. Hence, we must have

$$\rho_0 / \rho = J. \tag{2.10}$$

In order to see what form the conservation of mass takes across a discontinuity, we consider a disk-like volume enclosing the surface Σ, one base of which (S_1') is a surface parallel to Σ and a distance ϵ inside the original V_1, the other base (S_2') is another surface parallel to Σ and an equal distance inside the original V_2. The other bounding surface consists of a portion of a cylinder whose axis is perpendicular to a point on Σ. Let Σ' be the portion of Σ cut out by the cylinder. When we take the limit $\epsilon \rightarrow 0$, S_1' and S_2' approach Σ' and Eq. (2.8) becomes

$$dI/dt = -\int_{\Sigma'} [f(u^i - V^i)] \lambda_i d\Sigma = 0, \tag{2.11}$$

where now λ_i are the direction cosines of the normal to Σ drawn from the region V_1 to the region V_2. The square bracket is defined as in (2.9), and V^i are the components of velocity of Σ, that is, $V^i\lambda_i = V_n$.

Since (2.11) must hold for arbitrary Σ' in Σ, we must have as the law of conservation of mass across discontinuities

$$\rho_1(u_1{}^i - V^i)\lambda_i = \rho_2(u_2{}^i - V^i)\lambda_i = m. \tag{Ia}$$

The quantity m is the rate at which matter is crossing unit area of the discontinuity surface Σ.

The component of momentum in the x^i direction contained in a volume $V(t)$ is given by

$$\int_{V(t)} \rho u^i dV.$$

The law of conservation of momentum for a perfect fluid which has only normal pressures is contained in the statement

$$\frac{d}{dt}\int_{V(t)} \rho u^i dV = -\int_{S(t)} P^i dS = -\int_{V(t)} \frac{\partial P}{\partial x^i} dV,$$

where P is the pressure, and ponderomotive forces are assumed to be absent. A repetition of the argument given above leads to the equations

$$\rho\frac{du^i}{dt} + \frac{\partial P}{\partial x^i} = 0 \tag{II}$$

in regions of continuous flow and

$$(P_1 - P_2)\lambda^i = m(u_1{}^i - u_2{}^i) \tag{IIa}$$

across discontinuities, where m is given by (Ia).

Similarly, if U is the internal energy per unit mass of the gas, then the energy contained in the volume $V(t)$ is

$$\int_{V(t)} \rho(u^2/2 + U)dV.$$

The conservation of energy is contained in the statement that

$$d/dt\int_{V(t)} \rho(u^2/2 + U) = -\int_{S(t)} (Pu^i)\lambda_i dS.$$

The integral on the right-hand side of this equation is the work done by the fluid on the material outside the surface $S(t)$. By using the argument given above, this equation may be written as

$$\rho\frac{d}{dt}(u^2/2 + U) = -\frac{\partial(Pu^i)}{\partial x^i} \tag{III}$$

in regions of continuous flow and

$$m(u_1{}^2/2 + U_1) - m(u_2{}^2/2 + U_2) = P_1 u_1{}^i\lambda_i - P_2 u_2{}^i\lambda_i, \tag{IIIa}$$

across discontinuities.

Equations (I), (II), and (III) are the usual hydrodynamical equations describing continuous flow and (Ia), (IIa), and (IIIa) are the so-called Rankine-Hugoniot equations.[1] It is sometimes more convenient to replace Eq. (III) by a consequence of it and (I) and (II). Thus, multiplying Eqs. (II) by u^i and summing, we obtain

$$(1/2)\rho\frac{d}{dt}u^2 + \frac{\partial P}{\partial x^i}u^i = 0.$$

Subtracting this from (III) we obtain

$$\rho\frac{dU}{dt} + P\frac{\partial u^i}{\partial x^i} = 0.$$

In virtue of (I) this may be written as

$$\rho\left(\frac{dU}{dt} - \frac{P}{\rho^2}\frac{d\rho}{dt}\right) = 0.$$

Now from the first law of thermodynamics we have

$$TdS = dU + Pd(1/\rho),$$

where S is the entropy per unit mass. Hence, as a consequence of (I), (II), and (III) we have

$$\rho T(dS/dt) = 0. \tag{III$'$}$$

Equation (III′) is the statement that in a perfect fluid the entropy is constant, along a stream line which does not cross a discontinuity. The entropy may, of course, be different for different stream lines. That is,

$$S = S(\xi).$$

3. Consequences of the Rankine-Hugoniot Equations

If we multiply Eqs. (IIa) by λ_i and sum we obtain

$$P_1 - P_2 = m(u_1{}^\perp - u_2{}^\perp), \tag{3.1}$$

where $u^\perp = u^i\lambda_i$ and $u^\perp$ is the component of the particle velocity normal to the discontinuity. Thus the change in the velocity normal to the discontinuity is governed by Eqs. (3.1).

If we multiply Eqs. (IIa) by μ_i and sum where the μ_i are the direction cosines of any unit vector in the surface Σ (i.e., $\lambda^i\mu_i = 0$) we obtain

$$m(u_1{}^{\parallel} - u_2{}^{\parallel}) = 0. \tag{3.2}$$

Thus if $m \neq 0$ we see that the tangential components of the velocity are continuous across Σ.

Discontinuities for which $m = 0$ are possible and are called *slip streams*. It follows from (IIa) or (3.1) that for such discontinuities the jump in pressure is zero. Moreover, from (IIIa) it follows that the component

[1] See, for example, G. I. Taylor and J. W. Maccoll, *Aerodynamic Theory, Vol. III* (Verlag. Julius Springer, Berlin, 1935), edited by W. F. Durand, Div. H, p. 217.

of particle velocity normal to the discontinuity is continuous across it. From (3.2) it is evident that the component of velocity parallel to such a discontinuity need not be continuous.

In case $m \neq 0$ the discontinuity is called a shock or shock wave. In terms of the quantities $u^{\perp}$, $u^{\shortparallel}$ the Rankine-Hugoniot equations may be written as

$$m=\rho_1(u_1^{\perp}-V)=\rho_2(u_2^{\perp}-V) \tag{3.3}$$

$$P_1-P_2=m(u_1^{\perp}-u_2^{\perp}), \quad u_1^{\shortparallel}=u_2^{\shortparallel} \tag{3.4}$$

$$P_1u_1^{\perp}-P_2u_2^{\perp}=(m/2)\{(u_1^{\perp})^2-(u_2^{\perp})^2\}+m(U_1-U_2), \tag{3.5}$$

where V is the velocity of the shock normal to itself.

The first of Eqs. (3.4) may be written as

$$m\{(V-u_2^{\perp})-(V-u_1^{\perp})\}=P_1-P_2$$

or in consequence of (3.3) as,

$$m=\pm\left[(P_2-P_1)\Big/\left(\frac{1}{\rho_1}-\frac{1}{\rho_2}\right)\right]^{\frac{1}{2}}=\rho_1(u_1^{\perp}-V)=\rho_2(u_2^{\perp}-V). \tag{3.6}$$

Equation (3.5) may be written as

$$\tfrac{1}{2}(P_1+P_2)\left(\frac{1}{\rho_1}-\frac{1}{\rho_2}\right)=(U_2-U_1). \tag{3.7}$$

When the internal energy is known as a function of P and ρ, Eq. (3.7) determines the relation between P_2 and ρ_2 for known P_1 and ρ_1. Thus in the P, ρ plane (3.7) describes a curve through P_1, ρ_1, consisting of all states that can be attained from the given state P_1, ρ_1 by passing the gas through a shock. This curve will differ from the adiabatic through P_1, ρ_1 and hence the state P_2, ρ_2 will have a different entropy than that of the state P_1, ρ_1. In accordance with the second law of thermodynamics it will be possible to achieve by means of a shock only those states $P_2\rho_2$ for which the entropy is greater than the state P_1, ρ_1.

When U is a linear function of the temperature as is the case for a perfect gas, then the state P_2, ρ_2 will have greater entropy if and only if $P_2>P_1$, $\rho_2>\rho_1$. This follows from the fact that for a perfect gas we have

$$U=\frac{1}{\gamma-1}\frac{P}{\rho},$$

where γ is the ratio of the specific heats.

The states P_1, ρ_1 and P_2, ρ_2 could have been interchanged in the above argument since they enter the formula symmetrically. However, the gas must always be compressed in passing through the shock. Hence the sign to be used for m in Eq. (3.6) in front of the radical must be the same as the sign of P_2-P_1.

4. Viscosity and Heat Conductivity

If viscosity or heat conductivity or both are taken into account, then the discontinuity called the shock front is replaced by a continuous region of transition which propagates in the gas without changing shape. The "thickness" of this region will depend on the magnitudes of the viscosity and heat conductivity.

It can be shown that the transition region carries the gas from one constant state characterized by P_1, ρ_1, u_1, S_1 to another characterized by P_2, ρ_2, u_2, and S_2, where S_2,S_1 and the relations between the other quantities are those given by the Rankine-Hugoniot equations.

L. H. Thomas[2] has shown on the basis of the approximate value of the coefficient of viscosity and heat conductivity given by the simple kinetic theory of gases that the transition region even for very large changes in pressure is between one and two mean free paths and for moderate changes in pressure it is of the order of a few mean free paths.

In the remainder of this paper we shall ignore the viscosity and heat conductivity effects and consider a shock as a mathematical discontinuity in pressure, density, entropy, and particle velocity.

5. The Interaction Problem

It has been shown that due to the non-linearity of the hydrodynamical flow phenomena in a perfect fluid shocks develop. The properties of such discontinuities may be studied in terms of the phenomena occurring when they interact with boundaries of some sort in the fluid.

Two of the simplest types of boundaries that might be considered are density discontinuities or other shocks. One problem which may be considered as a limiting case of both of these is the problem of the oblique reflection of a plane shock from a rigid wall. It is obvious that the rigid wall may be considered as the limiting density discontinuity in which one medium has infinite density. Along the wall the velocity of the fluid must always be parallel to the wall. Thus, in the problem of the reflection of a shock wave from a rigid wall the effect of the wall is to specify that along a certain plane the fluid velocity is tangential to the plane.

If two plane shocks of equal strength intersect then from symmetry it follows that the flow of the fluid must be in the plane passing through the line of intersection of the shocks and bisecting the angle formed by the two forward moving sides of the shocks (see Fig. 1). Hence, the conditions in this plane are exactly those obtaining in the case of the reflection from a rigid wall. This problem is then mathematically identical with the problem of the reflection of a plane shock from a wall.

In such a problem there are two parameters available, namely the strength of the shock as measured by the

[2] L. H. Thomas, J. Chem. Phys. **12**, 449 (1944).

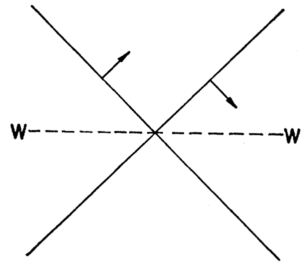

FIG. 1. The interaction of two equal plane shocks. The conditions along the plane WW are the same as those occurring in the reflection of an oblique plane shock from a rigid wall.

pressure jump, P_2-P_1 (or P_2/P_1) and the angle of incidence of the shock α. We shall define α as the angle between the normal to the incident shock and the normal to the wall. If the pressure jump is small the shock wave should behave as a sound wave, and it might be expected that some insight to the problem may be obtained from ordinary acoustic theory. However, that theory has the following very puzzling feature: If the "over-pressure" on the wall is plotted as a function of the angle of incidence then it is constant and equal to twice the "over-pressure" in the incident shock. If P_2' is the pressure behind the reflected wave,

$$P_2'-P_1=2(P_2-P_1)$$

for all angles of incidence except 90°. At 90°

$$P_2'-P_1=P_2-P_1.$$

Hence there is a discontinuity in this curve which does not seem reasonable. We shall see later (III-5) that there is a mechanism called Mach reflection which smooths out this discontinuity when the sound waves are considered as weak shocks.

The problem of reflection from a rigid wall may be considered as a steady-state phenomenon for some angles of incidence. Consider the region in the neighborhood of the intersection of the shock wave with the wall at any time. This region is unaffected by the past history of the reflection process when signals from points along the wall previously encountered by the shock wave move more slowly relative to the wall than does the shock wave. We shall see later that for a range of angles of incidence this is the case. For angles of incidence outside this range it is possible for the past history of the shock to influence it at any time.

6. Need for Experiments

In the foregoing discussion we have seen that when compressional disturbances of finite amplitude are propagated in a gas discontinuities develop. We have derived the differential equations which hold in regions of continuous flow and the conditions obtaining across discontinuities. In both cases the equations are the mathematical expression of the laws of conservation of mass, momentum, and energy. However, in deriving the mathematical expressions of these laws it was assumed that the microscopic view of a gas or fluid as a continuous medium was justified and that heat conductivity and viscosity could be neglected. The work of Thomas referred to in I-4 shows that these assumptions are approximately justified. However, the role that heat conductivity and viscosity play in various problems having to do with shock waves and their interactions can at present best be determined from experiment. Evidence exists which indicates that these effects cannot explain some experimental results which will be described in the following chapter.

In the theoretical discussion of the reflection of an oblique shock from a rigid wall, it is assumed that a reflected wave exists and that in the angular regions between the various shock waves and the wall the medium is in a uniform state. These assumptions reduce the mathematical problem to a purely algebraic one which will be discussed in some detail in Chapter III. It is worth noting that without them one would have to solve the differential Eqs. (I), (II), and (III) subject to the algebraic conditions (Ia), (IIa), and (IIIa) across discontinuities. The position and slope of all discontinuities other than that describing the incident wave would have to be determined from these equations and the boundary condition that the particle velocity at the wall must be tangential to the wall. The theory of such mathematical problems is in its infancy and hence one must resort to making various simplifying assumptions. Experiments can verify such assumptions, either directly or by verifying consequences of them.

We shall see that from photographic experiments on the reflection of oblique shocks all the evidence available at present verifies one set of simplifying assumptions only for limited ranges in the variables. Moreover, the situation which obtains for values of the variables outside these ranges is still obscure both from an experimental and a theoretical standpoint.

The remainder of this report will be concerned with the discussion of theoretical and experimental aspects of the problem of the reflection of a plane oblique shock from a rigid wall. This problem was first discussed by von Neumann.[3]

II. EXPERIMENTAL ASPECTS OF THE STUDY OF SHOCK WAVES

1. Experimental Methods

From the preceding discussion it is obvious that any method of producing a compression wave of large amplitude in a fluid having appropriate properties may be employed to create a shock wave. The early observations were made on the shock waves from explosions and the muzzle blast from guns. In the laboratory the condensed spark served as a useful source in much of the early work and was used by Mach in his historic experiments.[4] Detonation of small amounts of explo-

[3] J. von Neumann, "Oblique Reflection of Shocks," Explosive Research Report No. 12, Buord. U. S. Navy Department (October 1943).

[4] E. Mach, Akad. Wiss. Wien **77**, 819 (1878).

sives and sparks still represent the most convenient laboratory sources of spherical shock waves.

As soon as weapons employing supersonic projectiles came into use another source of shock waves was found in the bow wave emanating from the neighborhood of the nose of the projectile. Since firing a bullet at supersonic speeds is cheap and easy to do this means is often employed, especially since these shock waves have a direct bearing on supersonic flight.

The use of the wind tunnel is well known in aerodynamical studies and in recent times many supersonic tunnels have been constructed. These serve as excellent devices for the study of problems in steady flow but are very elaborate and expensive. Shock waves are also associated with the flow in high speed jets and nozzles and in recent times these devices have assumed great importance.

In speaking of useful sources of shock waves the water surface analogy should be mentioned.[5] It turns out that surface waves on water exhibit many of the properties of shock waves in a gas having a γ of two and therefore the scheme is a good analogy device for studying those properties of a gas which depend little on variations in γ.

A very convenient method of studying the transient effects of shock waves is that of the "shock tube." Since this paper deals almost exclusively with transient effects and the experimental data are mainly drawn from the shock tube and since it has been described only in rather inaccessible reports we include here a more detailed account of it and its use.

The propagation of waves of finite amplitude in tubes seems to begin with Davy[6] in 1816 followed by Bunsen in 1867. Berthelot and Le Chatelier both observed the high velocity of propagation in 1881 and Mallard and Le Chatelier obtained photographs of the phenomenon in 1883. In more recent times Payman[7] photographed explosions in tubes by an ingenious method. Most of the work mentioned above was concerned with the propagation of the explosion process in gases. Vielle[8] however observed that pressure waves of high velocity are created when a collodion or paper diaphragm separating a compression chamber from an expansion chamber was burst. This is exactly the principle on which the modern shock tube operates. Payman and Shepherd used this technique during World War II as did several people at Princeton University.[9] Unfortunately the reports of these latter efforts are rather inacessible.

[5] R. T. Knapp, *Analogy between Surface Shock Waves on Liquids and Shock in Compressible Gases* (Hydrodynamics Laboratory, California Institute of Technology, Pasadena, 1946).

[6] A survey of the early work is given by Dixon, Phil. Trans. **A200**, 315 (1903).

[7] W. Payman, Proc. Roy. Soc. **A120**, 90 (1928).

[8] P. Vieille, Comptes Rendus **129**, 1228 (1899).

[9] W. Payman and W. C. F. Shepperd, Proc. Roy. Soc. **A186**, 293 (1946). The work at Princeton is described in reports by G. R. Reynolds, OSRD No. 1519 (1943); Fletcher, Read, Stoner, and Weimer, OSRD No. 6321 (1946).

The shock tube of most interest in connection with the results to be discussed in this report is of uniform rectangular cross section so that plane windows may be installed flush with the inside of the wall for photographic investigations. It consists of two parts, the compression and expansion chambers which are of the same cross section and are clamped together in such a way as to hold a plane diaphragm between them. The expansion chamber is usually long compared to both its width and the length of the compression chamber. The windows in the expansion chamber are installed near the end remote from the diaphragm where observations may be made of the phenomena passing by. The compression chamber is then filled with a gas at pressure P_1 and the expansion chamber at a lower pressure P_0. The whole is allowed to come to temperature equilibrium T_0. If the diaphragm is suddenly burst (if made of Cellophane this may be accomplished by pricking it with a sharp point) a rarefaction wave is propagated into the compression chamber and a compression wave which turns into a shock propagates down the expansion chamber.

If it is assumed that the diaphragm is plane and disappears instantly and the shock wave is formed at this moment, a simple first-order theory of the tube may be applied.[9a] A temperature and density discontinuity occurs at the plane which separates the gas originally at pressure P_0 and now compressed to P from the gas originally in the compression chamber at P_1 and now expanded to the same pressure P. This plane moves with a velocity acquired by an element of the medium (the so-called particle velocity) in the expansion chamber when the shock wave passes over it and this must simultaneously be the velocity of an element of the medium in the compression chamber when the rarefaction wave passes over it. The situation is illustrated in Fig. 2. The particle velocity imparted by a shock wave is a known function of P/P_0. That imparted by the rarefaction wave is a different function of P_1/P_0. Equating these functions gives a relation between P/P_0 and P_1/P_0.

The particle velocity u acquired from the shock wave

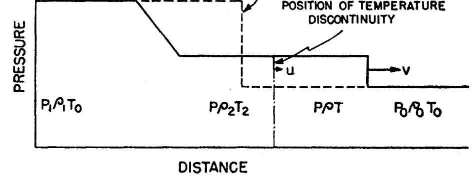

FIG. 2. The pressure distribution in a shock tube before and after the diaphragm is broken. The curve showing the pressure distribution in the gas passed over by the rarefaction wave is not a straight line but differs appreciably from one only when strong shocks are formed.

[9a] H. Schardin, Physik. Zeits. **33**, 60 (1932).

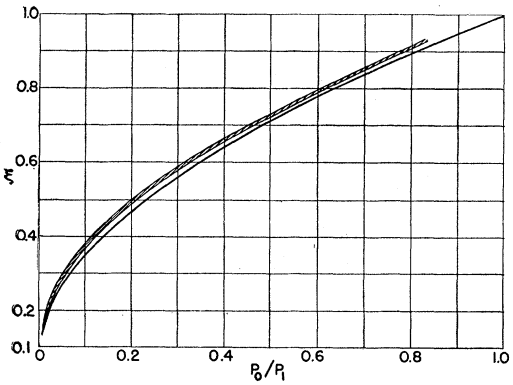

FIG. 3. Shock strength $\xi = P_0/P$ as a function of compression chamber pressure, P_1/P_0. The solid curve is a graph of Eq. (1.2). The shaded region covers experimentally observed results.

is obtained from the relations of Rankine and Hugoniot (Eq. (A7), Appendix A)

$$\frac{u}{c_0} = \left[\frac{2(y-1)^2}{\gamma[\gamma-1+(\gamma+1)y]}\right]^{\frac{1}{2}}.$$

Here c_0 is the velocity of sound in the undisturbed gas in the expansion chamber, γ is the ratio of specific heats of this gas, and $y = P/P_0$.

The velocity acquired by a particle from the rarefaction wave may be shown (see Appendix B, Eq. (B5)) to be

$$u/c_1 = [2/(\gamma_1 - 1)][1 - (yP_0/P_1)^{(\gamma_1-1)/2\gamma_1}],$$

where c_1 and γ_1 are the sound velocity and specific heats ratio, respectively, for the gas in the compression chamber. Equating the two expressions for u, we obtain

$$[yP_0/P_1]^{(\gamma_1-1)/2\gamma_1} = 1 - c_0(\gamma_1 - 1)(y-1)/ c_1[2\gamma\{\gamma - 1 + (\gamma+1)y\}]^{\frac{1}{2}}. \quad (1.1)$$

If air is in both chambers and if these are at the same temperature, $\gamma_0 = \gamma_1 = 1.4$, $c_0 = c_1$ and this equation may be written as

$$P_1/P_0 = y[1-(y-1)/(7+42y)^{\frac{1}{2}}]^{-7}$$
$$= (1/\xi)[1-(1-\xi)/\{\xi(7\xi+42)\}^{\frac{1}{2}}]^{-7}, \quad (1.2)$$

where $y = 1/\xi$.

It is evident from (1.1) that for a given value of y, P_1/P_0 is a function of the sound velocity ratio c_1/c_0 which decreases as c_1/c_0 increases, the amount of decrease depends on the values of γ and γ_1. Thus, by a proper choice of the gases in the two chambers greater shock strengths may be achieved for a given P_1/P_0. For example, if air is in both chambers $P_1/P_0 = 5.4$ for $y = 2.2$, while if helium[10] is in the compression chamber and if air is in the expansion chamber, $P_1/P_0 = 3.3$ for $y = 2.2$.

Now the ratio $y = P/P_0$ can be expressed in terms of the velocity of the shock wave (see Appendix A, Eq. (A5)).

$$(V/c_0)^2 = 1 + (\gamma+1)(y-1)/2\gamma. \quad (1.3)$$

One way, therefore, to determine the pressure in the shock wave is to measure its velocity and compute ξ or y from the above expression. This has been done a number of times at Princeton by different people during the war.[11]

A plot of the relation (1.2) is given by the solid curve of Fig. 3. The shaded region covers the experimentally observed results. It is expected that the theoretical curve should be too low since the diaphragm does not break in the ideal manner assumed.

From the simple theory of the tube one would expect the pressure immediately behind the shock front to be uniform. This is confirmed by experiments from two sources (1) photographic studies show no large changes in density behind the front provided sufficient time has elapsed for the front to assume a stable condition, and (2) measurements of the pressure with piezoelectric gauges verify the conclusion within their limits of accuracy. Figure 4 is a reproduction of an actual record obtained with a quartz gauge. Experience has shown that the oscillations in the record are to be ascribed to vibrations in the crystal mount rather than in the pressure itself.

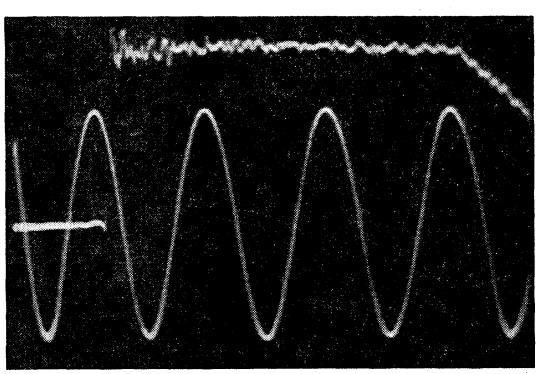

FIG. 4. A quartz gauge pressure-time oscillogram of a shock wave in the tube. The vertical displacement represents pressure. Also shown is a 1000-cycle sine-wave which determines the horizontal time scale.

A number of desirable qualities are now evident in this apparatus for the study of shock waves. (1) The tube gives a plane shock wave which is the type most amenable to mathematical analysis. (2) The result is a "step-function," i.e., the pressure is constant for some distance behind the shock front. (3) Within reasonable limits the shock is not attenuated as it passes down the tube.[12] (4) The shock and the flow behind it may be reproduced time after time with remarkable precision.

[10] The efficacy in using helium in the compression chamber was demonstrated by L. G. Smith at Princeton and more extensively by C. W. Mautz at the University of Michigan (to be published).

[11] See OSRD reports in reference 9.

[12] R. J. Emrich and F. B. Harrison, Phys. Rev. **73**, 1255(A) (1948).

(5) Boundary layer effects and turbulence seem to be vanishingly small for some distance behind the shock.[13]

Only two remarks will be made regarding the technique of operating the apparatus. The tube should be rather long so that little irregularities introduced at the time the diaphragm breaks have time to catch up and merge with the shock front before the point of observation is reached. The other is that the compression chamber should not be too short since the rarefaction reflected from the closed end catches up with the shock eventually and the region of constant pressure behind the shock then disappears. An interesting feature, mentioned only in passing, is the fact that the flow behind the shock may be made supersonic for sufficiently strong shocks and under these circumstances the flow behind the temperature discontinuity attains a high Mach number.

2. Methods of Measurement

The physical quantities which are of general interest in studying the interaction of shock waves consist of such things as temperature, density, pressure, and velocity of the medium, at all points in the field and the configuration in space and time of the discontinuities in these quantities. Simple techniques may be adequate if the phenomenon under investigation is stationary or quasi-stationary, since instruments may then be used which do not have rapid response. The Pitot tube, thermocouple, and hot-wire instruments are of this character and their use is so well known it is unnecessary to describe them here. The many photographic techniques may also be employed in quasi-steady flow without resorting to short duration light sources.

For transient phenomena devices having rapid response are needed. Useful instruments are the piezoelectric pressure gauge and the electrical strain gauge. These were used quite extensively during the war to measure the intensity of shock waves. As applied to the shock tube a quartz wafer or more usually a pair of wafers in a suitable mounting covered with a diaphragm or piston whose face is mounted flush with the inside surface of the tube gives good results. An insulated conductor separates the quartz plates and is connected through a suitable amplifier to a cathode-ray oscillograph. The rise time for the pulse recorded in this way is limited by the time required for the shock to pass over the face of the gauge which in practice is usually not smaller than 10^{-5} sec. This time is much shorter if the application is such that the shock is reflected normally from the face of the piston.

For the study of shock waves in the laboratory optical methods are by far the most powerful. One great advantage of such devices is that no disturbance to the flow is introduced by the observation itself. A second important consideration is resolving power, i.e., ability to sense changes in the variables over short distances, and in this respect the optical methods are unrivaled. Thirdly, if one uses a photographic technique a detailed map of the phenomenon may be covered in a single photograph for one instant of time and when coupled with sparks of short duration as sources of light, even the most rapid transient phenomena may be observed in great detail. The three most common optical arrangements are frequently referred to as shadow, schlieren, and interferometric, a brief description of which follows.[14]

The three optical arrangements are shown, respectively, in Fig. 5a, b, and c. The parallel shadow method consists of a small light source such as the pinhole at S, and collimating lens L_1 to cast parallel light on the photographic plate or screen P after having passed through the windows which enclose the region of interest. Disturbances in this region alter the uniform illumination originally falling on P. Reproductions of several photographs taken by this method will appear below.

In a typical schlieren arrangement, the pinhole is replaced by a slit or knife edge S_1 and lens L_2, knife edge S_2 and camera C are added. S_1 and S_2 are at conjugate foci and in operation S_2 is adjusted parallel to S_1 and advanced transversely until most of the light is cut off. The camera is focused on the region of interest between the windows. The medium under investigation may deviate light rays either toward or away from the knife edge, thus producing changes in the illumination of the plate. Illustrations of the use of this technique will be found in some of the figures which follow.

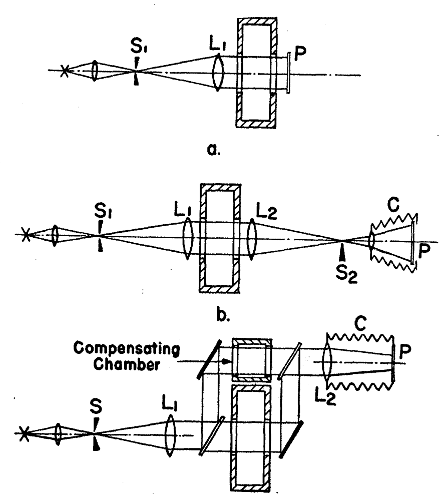

FIG. 5. A schematic diagram of the optical arrangement for (a) parallel shadow, (b) schlieren, and (c) interferometric photography.

[13] Evidence for this assertion is to be found, for example, in the sharpness of the slip stream in Fig. 10.

[14] A more detailed description of these methods may be found in the book by H. W. Liepmann and A. E. Puckett, *Introduction to the Aerodynamics of a Compressible Fluid* (John Wiley and Sons, Inc., New York, 1947).

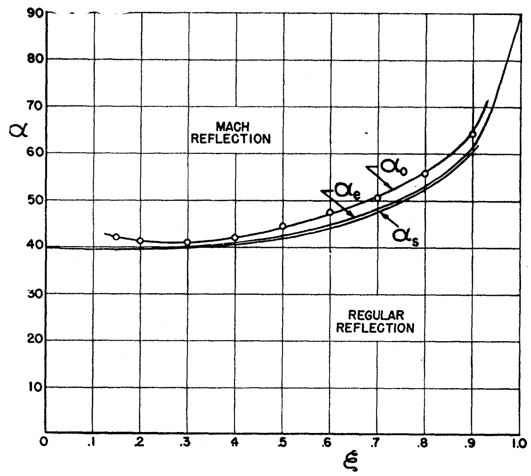

FIG. 6. Regions of regular and Mach reflection in the α, ξ (angle of incidence, shock strength) plane. The curve labeled α_e is the limiting curve above which regular reflection is theoretically impossible; that labeled α_s marks the boundary below which the past history cannot affect the reflection process, and that labeled α_0 marks the smallest α at which Mach reflection is observed.

The third technique interposes an interferometer in the light path as shown in C of the figure. The camera, again focused on the region of interest, forms a pattern of interference fringes on the screen P. Changes in density of the fluid between the windows induces shifts in the position of the fringes on the screen.

The theoretical aspects of these three methods of observation have been reviewed by Weyl.[15] When the deviation of an optical ray from its normal path in the absence of the disturbance can be treated as infinitesimal, he has shown that the interferometer measures the change in optical depth, that is, the integrated difference in local index of refraction. Under the same conditions the schlieren method is sensitive to the component of the gradient of the optical depth perpendicular to the knife edge while the shadow method responds to the second derivative of the optical depth. Essentially, therefore, the three techniques measure, respectively, the density, the first derivative, and the second derivative of the density.

The shadow method is cheap and easy to use and enables one to make quantitative measurements on the geometry of density discontinuities such as shock waves to which it is particularly sensitive. The schlieren arrangement is more elaborate and requires optical parts of high quality but it gives additional information about continuous variations of the density. Up to the present time the method has been used chiefly in a qualitative manner. Of the three methods the interferometric one is much the most elaborate and costly but it has many important advantages. Among these are quantitative evaluations of the density directly and high resolving power. It is the only optical method which has been used extensively to measure densities continuously over an extended region of a fluid in motion.[16] From the values of the density the behavior of the quantities such as pressure, temperature sound velocity, and flow velocity may be calculated from the equations discussed earlier.

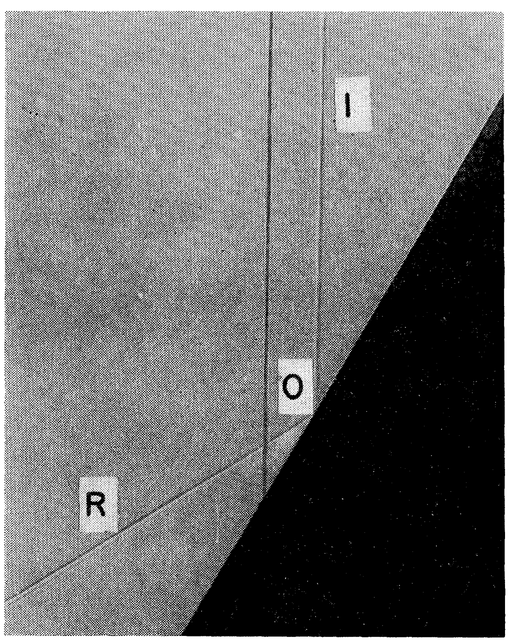

FIG. 7. A shadow picture of a regular reflection. The incident wave I is vertical and traveling to the right it makes an angle of 29° with the barrier which is represented in the figure by the solid black portion. The reflected wave R makes an angle of 27° with this barrier. The solid black line is a plumb line used for reference.

3. Results

A summary of all pertinent observations on the interaction of two shock waves is presented in this paper. Most of these data are taken from the work of Smith,[17] some from later experiments of our own and other sources as noted. Since most of the data come from studies of the reflection of shock waves from a wall a detailed description of the main features of this phenomenon is in order.

We shall discuss experiments involving a plane shock wave in air falling obliquely on a plane rigid wall and shall suppose that the phenomenon is viewed in the direction of their intersection. Observations are conveniently made by the parallel shadow method discussed earlier, the axis of the optical system having been adjusted parallel to the intersection of wall and shock. It is convenient to describe the results of such experiments in terms of two parameters. The first is the angle of incidence α which is defined as the angle

[15] F. J. Weyl, *Analytical Methods in Optical Examination of Supersonic Flow*, Navord Report 211-45, Buord. U. S. Navy Department.

[16] See, for example, Ladenburg, Winckler, and Van Voorhis, Phys. Rev. **73**, 1359 (1948).

[17] L. G. Smith, "Photographic Investigations of the Reflection of Plane Shocks in Air," OSRD No. 6271 (1945).

between the normals to the shock wave and the wall. The second is the shock strength which is defined as the ratio of the pressure ahead of the shock to that immediately behind it.

$$\xi = 1/y = P_0/P.$$

The observed effects can be divided into two main categories called "regular" reflection and "Mach" reflection. The situation may be described with the help of Fig. 6 where any point on the diagram corresponds to a particular choice of the independent parameters α and ξ. In air, regular reflection occurs for small α at all values of ξ. Let us fix our attention on a particular value of $\xi=\xi_1$ and note what happens to the reflection process as α goes from zero to 90°, that is, from head on to glancing incidence.

A typical example of the regular reflection observed for small α is shown in Fig. 7. This picture was taken in the shock tube by the parallel shadow method and represents the reflection of the shock from an inclined barrier placed across the tube between the two observation windows. The only observable features are plane incident and reflected shocks and it will be noted that the angle of incidence is not equal to the angle of reflection, $\alpha \neq \alpha'$. The speed with which the point of intersection O of the two shocks and the wall moves along the wall is given by $V/\sin\alpha$ where V is the velocity of propagation of the incident shock. Evidently this speed is very high and for sufficiently small α must be supersonic with respect to the medium behind the reflected shock. This means that the past history of the reflection process cannot influence its behavior in the future and to an observer moving with the point O a steady state exists in the neighborhood of this point.

In Fig. 8 is reproduced the result of a schlieren photograph of a similar reflection but α is now a little larger. We shall describe this figure in terms of an observer at rest with respect to the point O. A sound signal arising from the corner where the shock wave in the tube first struck the inclined barrier can be seen behind the reflected shock. That part of it which moves along the wall is behind the point O showing that the flow in this region is still supersonic with respect to the chosen observer. At some point along the reflected shock, however, the component of the flow perpendicular to the sound wave will be just sonic and beyond this point the shock wave is curved. This curvature can be ascribed to the influence of the sound wave.

An inspection of the schlieren photograph of Fig. 8 reveals that in the neighborhood of the point O there is no detectable departure from uniformity of the density in each of the angular domains formed by the two shocks and the wall. The theory of regular reflection given in III makes use of this result.

As the angle of incidence α in Fig. 6 is increased, the point at which curvature begins in the reflected shock moves closer to the point O. There is a critical value of α denoted here by α_s (for α-sonic) at which the sound

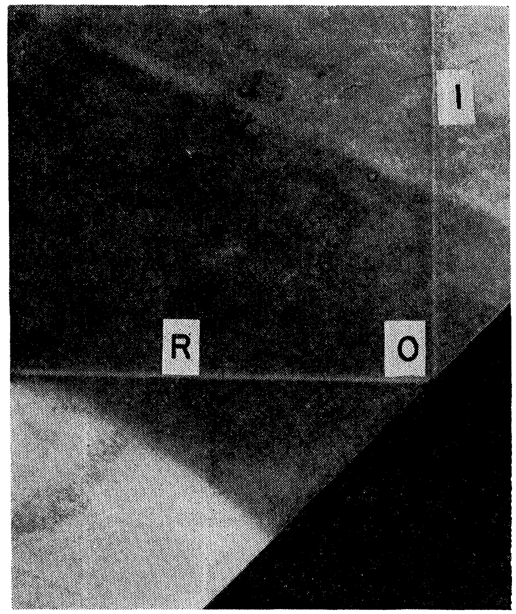

FIG. 8. A schlieren photograph of regular reflection. I and R are the incident and reflected shocks. The sound wave from the corner can be seen in the lower left-hand portion of the figure.

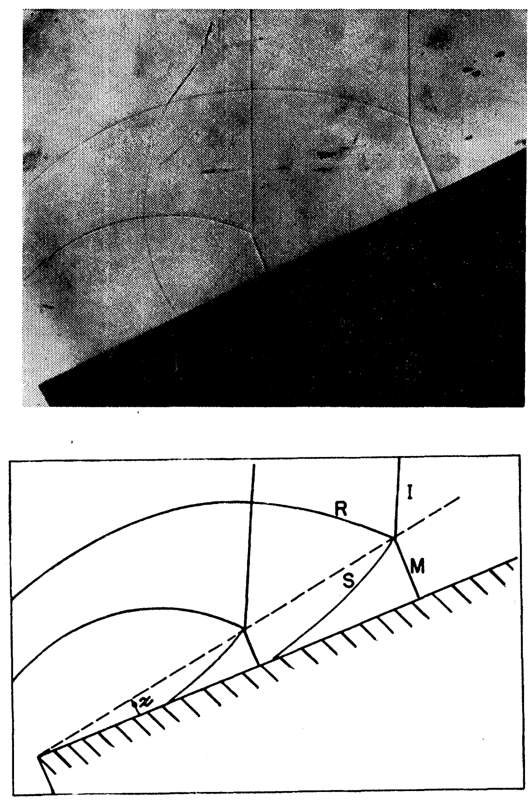

a

b

FIG. 9. A double exposure of Mach reflection by parallel shadow. 9a is the original and 9b is a tracing of the discontinuities. I, R, and M represent the incident, reflected, and Mach shocks and S represents the slip stream.

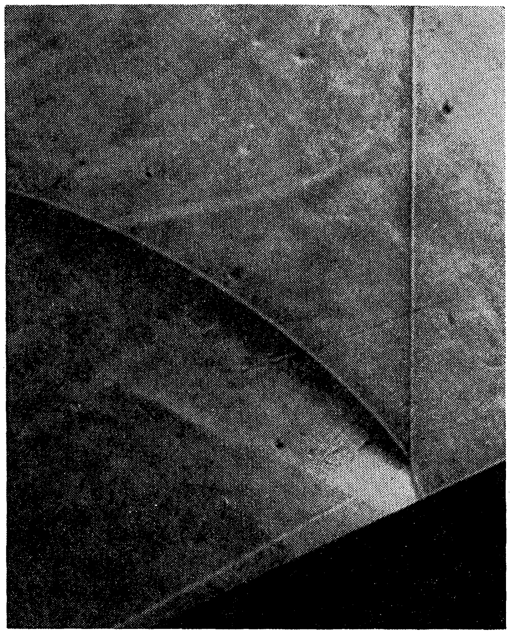

FIG. 10. A photograph of Mach reflection taken by the schlieren method.

wave extends to the point O and the flow behind this point is just sonic. The value of α_s can be computed as a function of ξ and α (see III, Section 6) and the lower curve of Fig. 6 is the result.

The distances traveled by the foot of the sound wave and the point O from the corner can be measured in the photographs. From the nature of the ratio of these distances as a function of α for fixed ξ, an experimental value for α_s can be determined. Smith[17] found good agreement between theory and experiment on this point.

Returning again to the sequence of phenomena observed as α is increased holding ξ constant, suppose that a large value of angle of incidence is chosen so that the point α, ξ_1 lies in the region labeled Mach reflection in Fig. 6. The photographs of Figs. 9 and 10 are typical of the shock configuration in this type of reflection. The reflected shock R now curved over its entire length intersects the incident shock I in a point T removed from the wall and a third shock M sometimes called

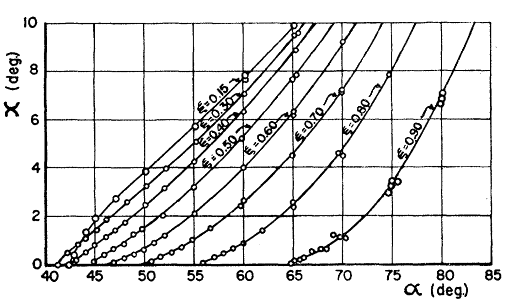

FIG. 11. Curves for the determination of the onset of Mach reflection.

the Mach shock extends from this point to the wall. The common point of intersection T of the three shocks will be referred to as the triple point.

In addition to the three shocks, and successive pictures confirm the fact that they are moving at supersonic speeds, there is visible a fourth discontinuity trailing behind the triple point. This is the slip stream marking the boundary between two regions of different density and temperature but the same pressure. Since the flow near the wall must be parallel to the wall and since the motion of the slip stream when lying in this region is inappreciable in the perpendicular direction, evidently this discontinuity cannot be a shock. Moreover, the existence of the slip stream is consistent with theoretical considerations of the problem, since the fluid which has been passed over by the two shocks I and R will undergo a smaller change in entropy than that which has passed through the single shock M. The total energy is the same on the two sides of the slip stream and hence the density and the fluid velocity are greater above this boundary while the temperature is greater below.

Experimentally the whole reflection phenomenon is very reproducible in the shock tube. For a given gas every feature of the configuration seems to be a definite function only of the parameters α and ξ to the precision with which the measurements can be made which is, to date, roughly one percent in ξ and one-tenth degree in α.

It should be remembered that the plane of the photographs is perpendicular to the line of intersection of the three shocks and every point on the photograph represents a projection of a line perpendicular to the sides of the shock tube. The phenomena are two-dimensional and, therefore, the state of affairs in all planes parallel to the photograph is the same.

It has been observed that the triple point which, of course, is the projection of the intersection of the four discontinuities, moves along a straight line passing through the corner and making an angle which we will call χ with the wall. In fact, if any point of the configuration having the plane radius vector r with the corner as origin is transformed to a new point cr where c is a scalar constant, a new configuration can be constructed corresponding to one physically observable. This means that instead of three independent variables (x, y, t) the phenomenon is describable in terms of two $(x/t,\ y/t)$. The variables x and y may be measured relative to any point moving with constant velocity with respect to the corner. In particular, they may be measured from T. Figure 9 is a double exposure of a Mach reflection in two different positions from which it may readily be verified that one Mach configuration is a dilitation of the other centered about the corner.

Experiment shows that for constant ξ the angle χ is an increasing function of α. As α decreases along a vertical line in Fig. 6 from a point in the region of Mach reflection, a critical value $\alpha=\alpha_0$ will be reached at which the Mach wave can no longer be detected and the triple point T seems to coincide with the wall. This angle α_0 is rather well determined by experiment by plotting χ *versus* α curves for constant ξ and extrapolating to $\chi=0$. Examples of such curves are shown in Fig. 11. The result of a whole series of such measurements is given by the upper curve in Fig. 6. The middle curve in this figure is a theoretical one giving the extreme angle α_e above which regular reflection is theoretically impossible. The derivation of this curve is given in III, Section 4.

Qualitatively, one can say that the regions of regular reflection below α_s and Mach reflection above α_0 have been fairly well mapped out experimentally and that below α_s an adequate theory, to be discussed presently, exists. There is no adequate theory of the Mach reflection as will be evident in the later sections of this report while between the curves α_s and α_0 both theory and experiment are confused.

Having given the broad features of the situation, it is now desirable to give a summary of the quantitative results which have been achieved by experiment. These consist at the present time[b] almost entirely of angle measurements as functions of the parameters α and ξ. However these data are so voluminous that we can find space for only a few typical series of observations in this review.

In presenting the data and in discussing their theoretical interpretation, it is convenient to make a transformation to a coordinate system in which the triple point T in Mach reflection or its counterpart O in regular reflection is at rest. Angles will be given with respect to the line joining the triple point and the corner which, in the case of regular reflection, is the boundary of the wall itself. In the actual experiments angles were measured from the wall but since χ is well defined and can be measured with precision the transformation introduces no significant errors. The four discontinuities I, R, M, and S of Fig. 12 make angles ω, ω', λ, and ϵ, respectively, at the triple point with the line TC. Also

$$\omega=\alpha-\chi, \quad \omega'=\alpha'+\chi,$$

and ω and ω' reduce to the angles of incidence and reflection for regular reflection ($\chi=0$). It will be noticed also that to the observer at rest with respect to T the incoming flow of the fluid is in the direction of the line TC.

A comparison between theory and experiment may be made by referring to Fig. 13. Data are plotted for the two shock strengths $\xi_1=0.8$ and $\xi_2=0.2$ representing weak and strong shocks, respectively. The solid curves were plotted from values computed by Polachek and Seeger[18] according to the theory outlined in III and IV, the curve labeled "two-shock theory" being one of the

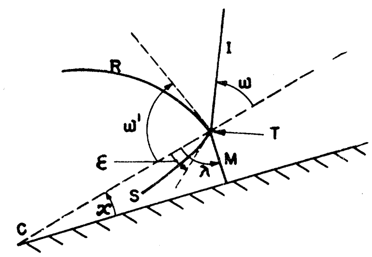

FIG. 12. Notation of angles used in Mach reflection. I, R, M, and S have the same significance as in Fig. 9b. C locates the position of the corner of the barrier shown by the shaded band.

family shown later in Fig. 15 of this report. The circles and crosses are experimental observations of regular and Mach reflections, respectively. The photographic plates were obtained and measured by Smith[17] and re-measured with some revisions by Harrison and Bleakney.[19] The revised points are plotted in Fig. 13. The decision on the point at which regular reflection ended and Mach reflection began was based on the extrapolation to $\chi=0$ of the curves of Fig. 11.

Figure 13 represents a small portion of the data available. Smith in his report gives similar plots for $\xi=0.9$ to 0.2 in one-tenth steps and a plot for $\xi=0.15$. In addition, he gives extensive data on all the other angles around the triple point.

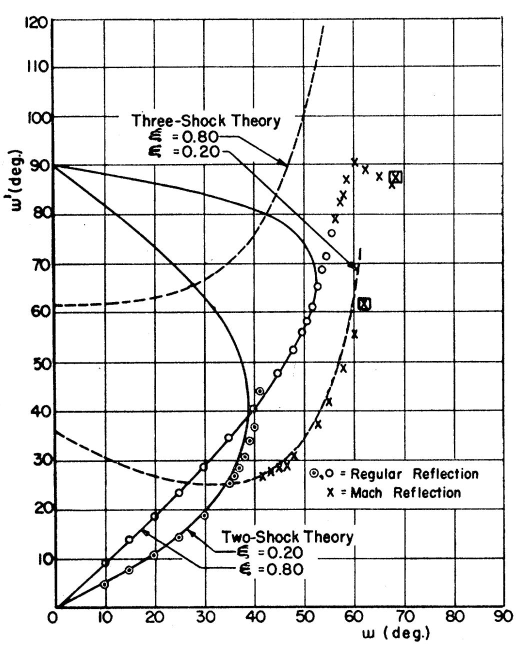

FIG. 13. Comparison of theory and experiment in regular and Mach reflection. The points enclosed in square boxes represent values of ω and ω' at which the total flow behind the incident shock is just sonic with respect to an observer moving with the triple point. There can be no solutions for ω greater than this limiting value.

[b] See, however, Appendix C.

[18] H. Polachek and R. J. Seeger, "Regular Reflection of Shocks in Ideal Gases," Explosives Research Report No. 13, BuOrd. U. S. Navy Department (1944).

[19] F. B. Harrison and W. Bleakney, "Remeasurement of Reflection Angles in Regular and Mach Reflection of Shocks Waves," Report to ONR, Contract N6ori-105, Task II (1947).

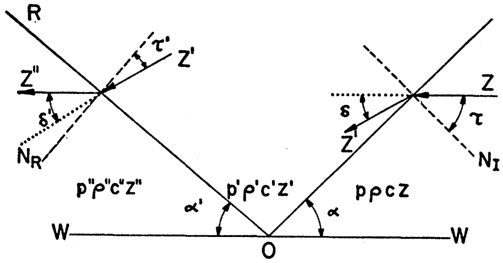

FIG. 14. Notation for theory of regular reflection.

There is good agreement between the theory of regular reflection and the observations for $\alpha<\alpha_e$ for all shock strengths ξ with one qualification. For the very strong shocks, $\xi\leq 0.2$, the points for α near α_e fall consistently below the two-shock curve. It is possible that some error may account for this but it seems unlikely. Seeger has suggested that the change in γ for air at high temperatures may be responsible.

For strong shocks the agreement of the observations for $\alpha>\alpha_0$ with the three-shock curve is not bad but certainly not as good as that for regular reflection. The deviations from the curve are consistent and above any normal experimental error.

Photographs taken by Ladenburg, Winkler, and Van Voorhis[16,20] in their study of jets show shock configurations similar to those observed in Mach reflection. Unpublished measurements on similar photographs by Ladenburg and Wachtell confirm Smith's results for ξ about 0.5 and ω of about 50°. For these values Smith found little disagreement with the three-shock theory. Ladenburg and Wachtell's angular measurements are not in complete agreement with this theory, but the disagreement cannot be considered as disproving the theory since the discrepancies are within the extremes of the experimental errors. The deviations found are in the same direction as Smith's.

Wind tunnel measurements[21] made at the National Physical Laboratory in England by G. H. Lean indicate a large discrepancy between three-shock theory and experiment for weak shocks and some agreement for strong shocks.

Both the jet and the wind tunnel experiments referred to here involve stationary three-dimensional shock configurations. The agreement of these experiments with those of Smith indicates that the configuration around the triple point is mainly determined by the flow in the immediate neighborhood of this point and does not depend greatly on the transient or stationary character of the flow.

Another feature to be noted in the results shown in Fig. 13 is that for weak shocks the points for Mach reflection seem to join on smoothly where regular reflection stops while for strong shocks there is a sharp discontinuity in ω' when Mach reflection begins. In all cases the experiments indicate that $\alpha_0>\alpha_e$, that is, regular reflection seems to persist beyond the angle of incidence at which the theory gives no solutions for regular reflection. Perhaps the strongest evidence pointing toward the inadequacy of the three-shock theory is to be found in the data representing Mach reflection for weak shocks where many of the points fall in a region where this theory predicts no solutions.

In view of the fact that the three-shock approach assumes that the state of the gas is uniform in the angular domains bounded by the discontinuities in the neighborhood of the triple point and in view of the wide discrepancies between theory and experiment, it is natural to look for departures from this basic assumption. Pictures of the reflection process taken by the shadow and schlieren methods have so far failed to reveal any angular variation in the density in the domains of interest. The schlieren pictures such as Fig. 10 seem to show some variations[c] immediately behind the reflected and Mach shocks, but these variations are not of the angular character one is lead to expect from the analysis given in Chapter IV.

Further discussion of the difficulties in explaining the results will be found in IV.

III. THEORY OF REGULAR REFLECTION

1. Introduction

We now turn our attention to the theoretical discussion of the regular reflection of a plane shock wave from a rigid wall. We shall assume in accordance with the experimental results for regular reflection that when a plane shock wave is incident upon a rigid wall a plane reflected shock is created and that in any of the angular domains involved the fluid is in a perfectly uniform state. Thus we effectively assume that the instantaneous situation is as in Fig. 14 where WW is the rigid wall, OI is the incident shock, and OR is the reflected shock. In the region WOI the fluid is characterized by the constant values of pressure, density, sound velocity, and particle velocity denoted, respectively, by P, ρ, c, and Z. In the region IOR we denote the corresponding quantities by a prime and in ROW by a double prime.

It is convenient to work in the coordinate system in which the point O is at rest. Then the assumption of constant conditions in each of the angular domains is equivalent to assuming that the phenomenon of reflection is stationary in this coordinate system.

The vectors Z and Z' denote the flow incident on and emergent from the incident shock wave I. We have already seen that the tangential components of particle velocity are conserved in crossing a shock wave. Moreover, the normal components are decreased since shock waves are compression waves and we must have

$$\rho u^{\perp}=\rho' u^{\perp\prime}.$$

[20] See also J. Winckler, Rev. Sci. Inst. 19, 307 (1948).
[21] G. H. Lean, "Report on further experiments on the reflection of inclined shock waves," National Physical Laboratory, London, 1946.

[c] See, however, Appendix C.

Hence the flow vector is deflected away from the normal to the shock crossing it. We shall denote the angle between the vectors Z and Z' by δ and call this the angle of deflection of the flow. It will be said to be positive if it is counterclockwise when measured as stated above. In Fig. 14, N_I and N_R are the normals to the incident and reflected shocks, respectively. The angle measured from the normal to a shock to the flow vector incident upon it is denoted by τ with or without a prime, depending on whether the shock is the incident or the reflected one. These angles are positive if they are counterclockwise when measured as stated. Thus in Fig. 14 τ and δ are positive and τ' and δ' are negative. The angle δ' is defined similarly in terms of the flow vectors Z', incident on the reflected shock, and Z'' emergent from it.

The problem of reflection of a plane shock is reduced by the assumption of constancy in the angular regions to that of given the angle of incidence, $\alpha=(\pi/2)-\tau$ and the strength of the incident shock, P'/P, to determine the position and strength of the reflected shock, that is, α' (or τ') and P''. The condition that must be satisfied is that the flow Z'' must be parallel to the wall. That is, we must have $\delta+\delta'=0$.

The Rankine-Hugoniot equations enable us to determine the deflections produced by a shock wave in terms of the strength of the shock and the angle of incidence of the flow. These will now be used to obtain the mathematical formulation of the condition that the total deflection be zero.

We shall do this in terms of the angles τ and τ'. It is evident from Fig. 14 that

$$\alpha+\tau=\pi/2, \quad \alpha'-\delta'-\tau'=\pi/2. \tag{1.1}$$

2. The Rankine-Hugoniot Equations

If z denotes the magnitude of flow vector Z incident upon a shock, then $z\cos\tau$ is the magnitude of the component of velocity normal to the shock and $(z/c)\cos\tau$ is the Mach number of this flow. The relation between pressure ratio and Mach number for a perfect gas with ratio of specific heats γ is

$$\frac{P'-P}{P}=\frac{2\gamma}{\gamma+1}\left[\left(\frac{z}{c}\right)^2\cos^2\tau-1\right].$$

If we set

$$x=\tan\tau, \quad y=P'/P.$$

This may be written as

$$y-1=\frac{2\gamma}{\gamma+1}\left[\left(\frac{z}{c}\right)^2\frac{1}{1+x^2}-1\right]. \tag{2.1}$$

The relation between pressure ratio and the compression ratio is given by

$$\eta=\frac{\rho'}{\rho}=\frac{(\gamma+1)y+\gamma-1}{(\gamma-1)y+\gamma+1}\geqslant 1$$

or, conversely,

$$y=\frac{(\gamma+1)\eta-(\gamma-1)}{(\gamma+1)-(\gamma-1)\eta}. \tag{2.2}$$

The two remaining Rankine-Hugoniot equations we take in the form

$$\left(\frac{z'}{c}\right)^2\cos^2(\tau+\delta)=\frac{1}{2\gamma}\left[\gamma-1+(\gamma+1)\frac{1}{y}\right] \tag{2.3}$$

and

$$\tan(\tau+\delta)=\eta\tan\tau. \tag{2.4}$$

Equation (2.3) is the statement that the relation between the Mach number of the flow emergent from a shock wave and the strength of a shock wave is that given by (2.1) with y replaced by $1/y$. Equation (2.4) is a consequence of the fact that tangential components of the flow are continuous whereas normal components are compressed in the ratio $1/\eta$. This equation may be solved to give

$$\Delta=\tan\delta=\frac{(\eta-1)x}{1+\eta x^2}. \tag{2.5}$$

Equations (2.1) to (2.5) hold across the shock I. The equations holding across R may be obtained from these by replacing each quantity properly. In our notation this is achieved by placing an additional prime on all quantities where

$$x'=\tan\tau', \quad \eta'=\rho''/\rho', \quad y'=P''/P'. \tag{2.6}$$

3. The Deflection Condition

The deflection by the reflected wave is given by

$$\Delta'=\tan\delta'=(\eta'-1)x'/(1+\eta'x'^2). \tag{3.1}$$

This equation may be written in terms of η, x, and x' alone, for η' is related to y' by the analog of (2.2) and y' is given in terms of x', η, and x by the analog of (2.1). Thus

$$y'-1=[2\gamma/(\gamma+1)][(z'/c')^2/(1+x'^2)-1].$$

Substituting from (2.3) for $(z'/c')^2$ we obtain after some algebraic manipulation

$$\eta'=\frac{(\gamma+1)B^2}{(\gamma-1)(B^2-1)+(\gamma+1)\eta}, \tag{3.2}$$

where

$$B^2=(1+\eta^2x^2)/(1+x'^2).$$

Hence (3.1) may be written as

$$\begin{aligned}\Delta'&=\frac{[2(B^2-1)-(\eta-1)(\gamma+1)]x'}{(\gamma+1)(1+\eta x^2)\eta-2(B^2-1)}\\&=\frac{[2(\eta^2x^2-x'^2)-(\eta-1)(\gamma+1)(1+x'^2)]x'}{(\gamma+1)(1+x'^2)(1+\eta x^2)\eta-2(\eta^2x^2-x'^2)}.\end{aligned} \tag{3.3}$$

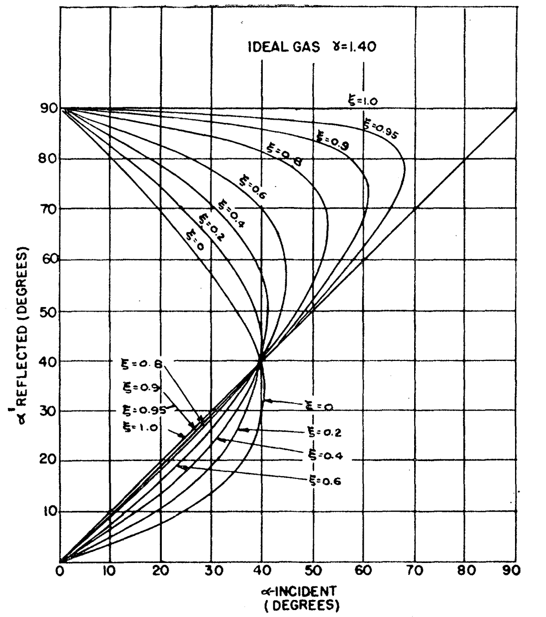

FIG. 15. Angle of incidence *versus* angle of reflection for shocks of different strengths undergoing regular reflection.

We are assuming that the reflected wave is a shock wave, that is $\eta'>1$. This condition gives us a limit for the possible values of x'; for it follows from (3.2) that $\eta'\geqslant 1$ if and only if

$$1+x'^2\leqslant 1+x_M'^2=\frac{1+\eta^2x^2}{1+(1/2)(\gamma+1)(\eta-1)}. \quad (3.4)$$

The values of x' obtained by using the equality sign are such that the reflected wave is just sonic.

If x and η are such that

$$\frac{1+\eta^2x^2}{1+(1/2)(\gamma+1)(\eta-1)}<1,$$

then the flow behind the incident wave is subsonic and no reflected wave can exist. If the inequality is replaced by an equality, the flow behind the reflected wave is sonic. The condition for this is

$$\cot\alpha=\tan\tau=x=(1/\eta)[(1/2)(\gamma+1)(\eta-1)]^{\frac{1}{2}}. \quad (3.5)$$

For angles smaller than τ given by (3.5) the assumed configuration can not exist. We shall then assume that τ is greater than this value.

The deflection condition is equivalent to the requirement that $\Delta+\Delta'=0$, that is, to

$$(\eta x-x')(\gamma+1)(1+x'^2)(\eta-1)(1+\eta x^2) \\ +2(\eta^2x^2-x'^2)(x'(1+\eta x^2)-(\eta-1)x)=0. \quad (2.6)$$

This is a cubic equation in x' from which we are to determine x' as a function of η and x. It is immediately evident that one root of this equation is

$$x'=\eta x>|x_M'|,$$

if $\eta>1$. Hence this root lies outside the limits obtained above and is not admissable. Dividing (3.6) by the linear factor $(\eta x-x')$, we are left with a quadratic equation for x' whose roots are negative and given by

$$x'=\frac{-x(1+\eta^2x^2)\pm[x^2(1+\eta^2x^2)^2-(1+\eta x^2)((\gamma+1)(\eta-1)+2)(\eta-1)((\gamma-1)(1+\eta x^2)+2)]^{\frac{1}{2}}}{(1+\eta x^2)(\gamma+1)(\eta-1)+2}. \quad (3.7)$$

From Eqs. (3.7), (3.1), and (1.1) we can compute α', the angle between the normal to the reflected wave and the normal to the wall, as a function of $\xi=1/y$, and α. Graphs of these functions for $\xi=0.8$ and $\xi=0.2$ are given on the curves labeled "two-shock" in Fig. 13. The upper portions of these curves correspond to the use of the plus sign in front of the radical in (3.7), the lower portion to the minus sign. Figure 15 taken from the report of Polachek and Seeger[18] gives a set of curves each of which represents α' as a function of α for the fixed value of ξ given on the curve and $\gamma=1.4$.

Thus there are two possible positions for the reflected shock. For each of these we may compute the pressure behind the reflected wave by computing η' from Eq. (3.2) and y' from the analog of (2.2). It is evident from their equations that η' and y' are monotonic increasing functions of B^2 for fixed η and hence monotonic decreasing functions of x'^2. Hence for the root given by the plus sign in Eq. (3.7) the pressure on the wall is greater than for that given by the minus sign. Moreover as η approaches one, that is, the incident wave becomes sonic, the root given by the plus sign approaches zero and the pressure on the wall approaches infinity whereas that given by the minus sign approaches $-x$ and the pressure on the wall remains finite. Thus in this limiting case the root given by the plus sign seems contrary to the predictions of the acoustic theory and must be discarded. It is to be expected that it is also to be discarded when η is appreciably different from one. In the various experiments on regular reflection the measurements show that the position of the reflected wave is always that corresponding to that given by the minus sign in front of the radical in Eq. (3.7). The heuristic reasoning given above seems to be borne out by experiment.

4. The Extreme Angle

When

$$x^2(1+\eta^2x^2)<(1+\eta x^2)(\eta-1)((\gamma+1)(\eta-1)+2) \\ \times((\gamma-1)(1+\eta x^2)+2), \quad (4.1)$$

the roots given by (3.7) become complex. Hence the assumed configuration is impossible for such values of x and η. That is, there is no position of the reflected wave within the sonic lines $x'=\pm|x_M'|$ such that the total deflection of the flow is zero. The experiments show that for most angles of incidence and shock strengths such that the inequality (4.1) holds, Mach reflection takes place.

When the inequality sign in (4.1) is replaced by an equality sign we obtain a condition for the smallest value of τ, and hence the greatest value of α, the angle of incidence, for which the two shock configuration is possible. We shall call these angles τ-extreme and α-extreme, respectively. We have called the region in the η, τ or ξ, α plane where the two-shock configuration is found experimentally the region of regular reflection. A theoretical boundary of this region is given by

$$x^2(1+\eta^2x^2)=(1+\eta x^2)(\eta-1)((\gamma+1)(\eta-1)+2)\times((\gamma-1)(1+\eta x^2)+2). \quad (4.2)$$

This may be rewritten as

$$1+\eta x^2=\frac{-(1-2\eta(1+A))+[(1-2\eta(1+A))^2-4\eta(1-A(\gamma-1)(\eta-1))]^{\frac{1}{2}}}{2\eta(1-A(\gamma-1))}, \quad (4.3)$$

where

$$A=(\eta-1)(2+(\gamma+1)(\eta-1)).$$

The positive sign must be taken in front of the radical since $1+\eta x^2$ must be positive.

In the case of weak shocks we may write $\eta=1+\epsilon$ and neglect higher powers of ϵ than the first. Then,

$$\begin{aligned} x^2&=2\epsilon(\gamma+1)=2(\gamma+1)(y-1)/\gamma,\\ \tau&=(\pi/2)-\alpha=[2(\gamma+1)(y-1)/\gamma]^{\frac{1}{2}}. \end{aligned} \quad (4.4)$$

This gives the angle of incidence for weak shocks at which regular reflection is theoretically no longer possible.

5. Sonic Angle

In the region of regular reflection, the two-shock configuration is determined as above for a given incident shock strength and angle of incidence less than the extreme angle. We now consider the Mach number of the flow behind the reflected shock, namely, z''/c'' where

$$(z''/c'')^2=(1+\eta'^2x'^2)[(\gamma-1)y'+(\gamma+1)]/2\gamma y'. \quad (5.1)$$

In this expression η', x', and y' are known functions of η and x. Hence for each η we may determine the value of x such that $z''/c''=1$. The corresponding value of τ and α denoted by τ_s and α_s will be called the *sonic angle.* If this condition is satisfied, signals sent out at points along the wall as the incident wave passes over these points will travel along with the point of intersection of the incident shock wave and the wall.

This angle is plotted as a function of α and $\xi=1/y$ for $\gamma=1.4$ (air) in Fig. 6. It is evident from this plot that α_s is less than one degree smaller than α-extreme.

For angles of incidence less than α_s it is evident that the assumption, that the flow is stationary in the coordinate system in which the line of intersection of the incident shock and the wall is at rest, is correct. In such a case $z''/c''>1$ and signals cannot reach this point. Hence the reflection process cannot be influenced by its past history. However if α is greater than α_s the stationary assumption has no real justification and the phenomenon may be transient.

6. Pressure Behind the Reflected Wave

In II, Section 5, it was pointed out that the usual acoustic theory determines the dependence of pressure behind the reflected wave as a function of the angle of incidence α and that this function is discontinuous at $\alpha=90°$. If we regard sound waves as weak shocks we may replace acoustic theory by that developed above. We then find that at values of α near 90°, i.e., values of α greater than that given in (4.4), the assumption of two shocks in the reflection process is an impossible one. Thus, the usual acoustic theory is not valid near $\alpha=90°$ and the discontinuity in the pressure behind the reflected wave as a function of the angle of incidence must not be taken seriously. Presumably the mechanism of Mach reflection smooths out this function so that the excess pressure behind the reflected wave varies smoothly from twice the excess pressure behind the incident wave to one times this value. However, for weak shocks and for angles of incidence near and less than α-extreme the excess pressure behind the reflected wave can be calculated to be approximately three times the excess pressure behind the incident wave. Thus the transition provided by the Mach reflection seems to smooth out the discontinuity mentioned by introducing a sharp maximum around α-extreme.

Von Neumann was the first to point out these facts about the pressure behind the reflected wave as a function of the angle of incidence. His discussion, which uses different variables, may be found in Navy reports.[3] In terms of the notation used here, these results may be obtained as follows: From the analog of Eqs. (2.1) we have

$$\begin{aligned}(P''/P')-1=\xi'-1&=[2\gamma/(\gamma+1)][z'^2/c'^2(1+x'^2)-1]\\ &=[2\gamma/(\gamma+1)][(z'/c')^2(1+\eta^2x^2)\\ &\quad\times\cos^2(\tau+\delta)/(1+x'^2)-1].\end{aligned}$$

Substituting from (2.3) for z'/c' and performing some algebraic manipulation, we obtain

$$P''/P=1+(B^2-1)(1+y(\gamma-1)/(\gamma+1).$$

This equation gives the pressure behind the reflected

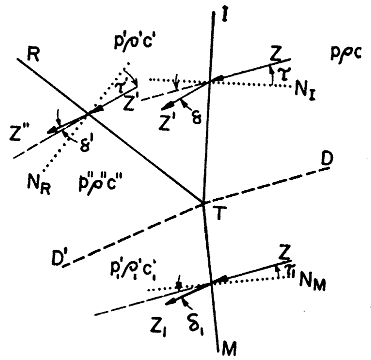

FIG. 16. Notation for the theory of Mach reflection.

wave as a function of x and η as soon as x' is determined from (3.7) and substituted into B^2.

For weak shocks when x is given by (4.4), we have

$$x' = -\frac{x}{2}\left[1-\frac{(\gamma+1)}{2}\epsilon\right]$$

$$B^2-1=\tfrac{3}{4}x^2=3(\gamma+1)(y-1)/2\gamma$$

and hence

$$(P''/P)-1=3(y-1).$$

7. Summary

We have thus seen that for each value of ξ or η there is an angle α-extreme denoted by α_e such that for $\alpha<\alpha_e$ the two-shock theory has two solutions for the position and strength of the reflected wave. For $\alpha=\alpha_e$ these two solutions coincide and for $\alpha>\alpha_e$ there are no real solutions. Thus the curve given by α_e as a function of ξ divides the ξ, α-plane into two parts which overlap the regions we have called *regular reflection* ($\alpha<\alpha_s$) and *Mach reflection* ($\alpha>\alpha_0$), where $\alpha_s<\alpha_e<\alpha_0$.

In the discussion of the experimental results given above, it was pointed out that the theory of regular reflection was verified for all angles of incidence less than α_s, and that Mach reflection seems to take place for angles of incidences greater than α_0. The band in the ξ, α-plane given by $\alpha_s\leq\alpha\leq\alpha_0$ includes the angle α-extreme. The resolving power of experiments performed to date is not great enough to determine where in this narrow band the onset of Mach reflection takes place.

The remarkable agreement between theory and experiment for regular reflection for shocks of all strengths (with the possible exception of some cases for $\xi=0.20$ and $\xi=0.15$) would seem to verify the assumptions made in the theory. In particular, this seems to justify the neglect of viscosity and heat conductivity in these cases. We shall find that by making similar assumptions in the case of Mach reflection the theory obtained disagrees at times very violently with experiments. The theories to be discussed briefly below have been criticized because they do not take heat conductivity and viscosity into account. It may be that this is a crucial defect. However, if these played an important role one would expect that some evidence of this would be found in the comparison of theory and experiments in the case of regular reflection.

IV. THEORETICAL ASPECTS OF MACH REFLECTION

1. Introduction

The experimental result that the triple point of a Mach configuration travels along a straight line making an angle χ with the corner was anticipated theoretically by von Neumann from simple arguments based on dimensional analysis. Since there is no length inherent to the problem if heat conductivity and viscosity are ignored, new solutions of the hydrodynamical equations can be obtained by replacing the variables (x, y, t) in one solution by (sx, sy, st) for arbitrary s. If, as seems to be the case experimentally, a unique solution is to exist then all these solutions must be the same. That is, the transformation $(x, y, t)\rightarrow(sx, sy, st)$ must leave the solution unaltered. Thus the dimensionless quantities involved must be functions of x/t and y/t.

This experimentally verified result implies that if at any time t there exists a small region around the triple point in which the variables such as pressure or density are independent of distance from the triple point, then at later times the size of this region will expand in proportion to the time interval. The functions describing the flow around the triple point are of course singular at T. If this singularity is such that in a region around T at some time the flow is independent of the distance from the triple point, then for later times (and earlier ones) in different sized regions the flow variables must depend only on an angle variable measured around T. If the curvature of one of the various discontinuities meeting at T increased indefinitely as one approached T along the discontinuity, then one would not expect the assumption regarding independence of the flow with distance to hold at any time. There may of course be other reasons for discarding this assumption.

The resolving power of the existing experiments is insufficient to decide definitely whether the curvature of the discontinuities other than the incident shock is finite at T. The measurements by Bleakney and Harrison of Smith's photographic plates gave slightly different results from Smith's original values which can be ascribed to different methods of estimating the final finite curvatures. However, it is possible that new experiments with better resolving power may indicate that the change of curvature of the discontinuities near the triple point increases markedly. This may explain the paradoxical situation with which we are now faced and which will be described below.

2. Three-Shock Theory

We begin with the assumption that not only does there exist a region around T where the flow variables are independent of distance from T but also that in this region the flow variables are constant in each of the angular domains around T delineated by the various discontinuities. This strong assumption seems to be borne out by the schlieren photographs of which Fig. 10 is a typical example. It is, of course, a natural assumption to make in view of the success of the two-shock theory and has the virtue that it reduces the theoretical discussion to an algebraic problem. However, it has the fault that it deals only with local aspects of the flow around the point T and hence it cannot give any prediction as to the value of the angle χ for an incident shock with a given α and ξ.

Thus we assume that three plane shocks all meet in a line and see how such a configuration is to be determined in terms of the strength of one, called an incident one, and the angle of mass flow incident upon this shock. The notation will be a simple extension of that used in Fig. 14. Figure 16 illustrates the shock configuration assumed in the coordinate system in which the line of intersection of the three shocks is at rest.

The line TI represents the incident shock, TR the reflected shock, and TM a third shock which we will call the Mach shock. The line TD represents the direction of the flow incident on TM and TI (the path of the triple point) and the line TD', the slip stream represents the flow emergent from T. In the angular regions MTI, ITR, RTD', $D'TM$ all quantities of interest will be assumed to be constant. This is the stationary hypothesis. The pressure, density, sound velocity, and particle velocity in the region MTI will be denoted by P, ρ, c, and Z. In the region ITR they will be denoted by the same letters with a prime, in RTD' by the same letters with a double prime and $D'TM$ by the same letters with a subscript 1 and a prime. The lines N_I, N_R, and N_M are the normals to the incident, reflected, and Mach shock, respectively.

If only three shocks are to be present we must have

$$P''=P_1'. \tag{2.1}$$

We shall denote as in the two-shock case the angle between the normal to a shock and the flow incident upon it by τ with appropriate primes and subscripts to distinguish between shocks. Similarly the angles of deflection of the flow will be denoted by δ with suitable primes and subscripts.

In addition to the requirement (2.1) we must have

$$\delta_1=\delta+\delta'. \tag{2.2}$$

The two conditions (2.1) and (2.2) serve to determine the allowed configurations in terms of τ and ξ (or η). The explicit formulas may be obtained by specializing the formulas given by Taub[22] in a paper on refraction of shock waves.

The solution is again not unique. For example, one possible solution may always be obtained by assuming that TM is a continuation of TD and that TR is a sound wave ($\eta'=1$). Such solutions will be called trivial ones.

Solutions of these equations have been given by Polachek and Seeger.[18] The results of one family of such solutions are plotted in Fig. 13 as the curves labeled "three shock." Other families exist but they have not been considered seriously because of heuristic arguments such as those given in III, Section 3, for discarding one solution of the two-shock theory. The experimental results seem to come closest to the solutions plotted and this gives a justification of sorts for discarding the others. There is one feature of these solutions which can be proved analytically and which is important for comparison with experiment. It is the following: There exists a value for ω corresponding to ω_e in the two-shock theory such that for ω larger than this value no non-trivial solutions to the three-shock equations exist. Moreover, for weak shocks this value is smaller than ω_e for the two-shock theory.

It has been pointed out earlier that the experiments on Mach reflection, especially those involving weak incident shocks are in disagreement with the three-shock theory. The most violent disagreement is that Mach reflections exist where there are no non-trivial solutions for the three-shock configuration.

3. Prandtl-Meyer Variations

We have seen that if we weaken the uniformity assumption we can only admit angular variations in the state of the fluid around the triple point unless we are willing to admit some violent singularity at T such as infinite curvature of the discontinuities. Continuous angular variations in the state of a compressible fluid are known as Prandtl-Meyer variations and the equations describing them are given by Taylor and Maccoll.[1] They have the property that the component of the flow normal to the radius vector is always sonic. Moreover, the radial component increases outward in such a variation and the flow is always turned toward the point around which angles are measured.

It can be shown from these properties that the Prandtl-Meyer variations cannot follow the Mach shock but can exist in the other angular regions involved. It is, of course, natural to assume that they do not precede the incident shock. Bargmann and Montgomery[23] found solutions for the equations describing a configuration of three shocks and a Prandtl-Meyer variation following the reflected shock for $\xi=0.8$ and all values of ω between ω_e and the value of ω corresponding to glancing incidence. They failed to find any for a configuration in which a Prandtl-Meyer variation preceded the reflected shock but did find solutions for a configuration in which it preceded the Mach shock. The values of the angles computed in the last case

[22] A. H. Taub, Phys. Rev. **72**, 51 (1947), Eqs. (7.5), (7.3), and (5.6) with $\gamma_1=\gamma$ and $\Gamma=1$.

[23] V. Bargmann and D. Montgomery, "Prandtl-Meyer Zones in Mach Reflection," OSRD No. 5011.

agreed with Smith's experimental values much better than did those of the first case.

Thus some measure of agreement with experiment may be achieved by inserting Prandtl-Meyer variations in the configuration. However, the best agreement is obtained by placing them in a region where it is difficult to conceive of how they can be formed. Moreover, the schlieren photographs show no signs of angular variations in this region. As mentioned earlier, no evidence of these variations have been found in any region to date. Here again improved resolving power may throw further light on the matter.

It is apparent that a complete solution of the hydrodynamical problem of Mach reflection is beset with very great difficulties. However, the special case of nearly glancing incidence has been solved by Bargmann[24] but at the time of this writing no experimental data are available[d] for comparison with the theory.

The present situation regarding Mach reflection may be summarized as follows. The mass of experimental data accumulated cannot be explained by any existing theory. The assumption of uniformity in the various domains in the neighborhood of the triple point is in disagreement with experimental results. However, there is no experimental evidence at present for the existence of the only types of variations which seem to be possible, namely, angular variations. It is hoped that future experiments using interferometric optical methods will either discover such variations or disclose the nature of the singularity at the triple point and give a better understanding of the phenomena involved in the interactions of shocks.[25]

APPENDIX A. CONSEQUENCES OF THE RANKINE-HUGONIOT EQUATIONS

In this appendix we derive some consequences of the Rankine-Hugoniot Eqs. I (3.6) and I (3.7) which have been used in the text. We shall assume that we are dealing with a perfect gas and shall first express the shock velocity, the change in particle velocity, and the ratio of the density behind the shock to that in front as functions of the ratio of the corresponding pressures. The subscript 1 will denote a quantity in front of the shock and the subscript 2 will denote a quantity behind the shock.

For a perfect gas Eq. I (3.7) may be written as

$$\tfrac{1}{2}(P_1+P_2)\left(\frac{1}{\rho_1}-\frac{1}{\rho_2}\right)=\frac{1}{\gamma-1}\left(\frac{P_2}{\rho_2}-\frac{P_1}{\rho_1}\right)$$

or as

$$\eta=\frac{(\gamma+1)y+\gamma-1}{(\gamma-1)y+\gamma+1}, \tag{A1}$$

where

$$\eta=\rho_2/\rho_1, \quad y=P_2/P_1. \tag{A2}$$

As y varies from 1 to ∞, η varies from 1 to $(\gamma+1)/(\gamma-1)$. For $y=1+\epsilon$ where ϵ^2 may be neglected relative to ϵ, we have

$$\eta=1+(1/\gamma)\epsilon$$

which agrees with the adiabatic curve. Note that if in (A1) y is replaced by $1/y$ then η is replaced by $1/\eta$.

One of Eqs. I (3.6) may be written as

$$(V-u_1{}^{\perp}/c_1)^2=(y-1)/\gamma(1-1/\eta)$$

where c_1 is the velocity of sound in front of the shock, i.e.,

$$c_1{}^2=\gamma P_1/\rho_1.$$

Substituting for η as a function of y we obtain

$$[(V-u_1{}^{\perp})/c_1]^2=(1/2\gamma)[(\gamma+1)y+\gamma-1]. \tag{A3}$$

Using the other Eq. (3.6) we obtain

$$\begin{gathered}[(V-u_2{}^{\perp})/c_2]^2=(1/2\gamma)[(\gamma+1)/y+\gamma-1]\\ c_2{}^2=\gamma P_2/\rho_2.\end{gathered} \tag{A4}$$

The quantities on the left of these equations is the square of the speed of the shock wave relative to the medium in front of the shock and behind the shock, respectively, divided by the velocity of sound. These quantities are also the Mach numbers of the flow ahead and behind the shock relative to the shock wave. We thus have the result that the Mach number behind the shock is the same function of $1/y$ as the Mach number ahead of the shock is of y. Equation (A3) may be written as

$$M_1{}^2-1=\frac{\gamma+1}{2\gamma}(y-1) \tag{A5}$$

$$M_2{}^2-1=\frac{\gamma+1}{2\gamma}(1/y-1). \tag{A6}$$

From these equations and the fact that $\gamma>1$ and $y\geqslant 1$ it is evident that $M_1\geqslant 1$ and $M_2\leqslant 1$.

Equation I (3.6) may also be written as

$$[(u_2{}^{\perp}-u_1{}^{\perp})/c_1]^2=(1-1/\eta)^2(V-u_1)^2/c_1{}^2,$$

substituting from (A1) and (A3) we obtain

$$[(u_2{}^{\perp}-u_1{}^{\perp})/c_1]^2=2(y-1)^2/\gamma[(\gamma+1)y+\gamma-1] \tag{A7}$$

as the expression for the change in particle velocity in passing through the shock as a function of y.

In terms of the Mach number M_1 of the shock we may write (A7) as

$$(u_2{}^{\perp}-u_1{}^{\perp})/c_1=[2/(\gamma+1)][M_1-1/M_1]. \tag{A8}$$

---

[24] V. Bargmann, "On Nearly Glancing Reflection of Shocks," AMP Report 108.2R National Defense Research Committee (March 1945).

[d] See, however, Appendix C.

[25] A discussion of some of the problems treated in this review is to be found in a paper by H. Polachek and R. J. Seeger, "On Shock Wave Phenomena: Interaction of Shock Waves in Gases. Non-Linear Problems in Continua," Proceedings of Symposia in Applied Mathematics, Vol. I, American Mathematical Society, New York (1949) (in press).

This follows from the equation before (A7) on substituting for η from (A1) and for y from (A5).

From the definitions of c_1 and c_2 and the relations derived above we have

$$(c_2/c_1)^2 = y/\eta = y[(\gamma-1)y+\gamma+1]/[(\gamma+1)y+\gamma-1]. \quad \text{(A9)}$$

APPENDIX B. SIMPLE SOLUTIONS OF THE EQUATIONS OF MOTION

In this appendix we derive the corresponding results for a one-dimensional rarefaction wave which we assume carries the medium from one constant state denoted by the subscript 1 to another denoted by the subscript 2. In this case there are no discontinuities in the flow and if we assume that all the medium ahead of the disturbance is at the same entropy it will remain so. Hence the relation corresponding to (A1) is the equation of the adiabatic for the gas:

$$P_2/P_1 = (\rho_2/\rho_1)^\gamma. \quad \text{(B1)}$$

The velocity and pressure profiles in the disturbed region are not constant in this case. Each portion of the profile moves relative to the medium around it with a speed given by the velocity of sound at that portion of the medium. Thus the beginning and the end of the disturbed regions move with velocities c_1+u_1 and c_2+u_2, respectively, where c_1 and c_2 are given by

$$c_1^2 = \gamma P_1/\rho_1, \quad c_2^2 = \gamma P_2/\rho_2 \quad \text{and in general } c^2 = dP/d\rho, \quad \text{(B2)}$$

respectively.

In order to determine u_2 we must discuss the differential equations expressing the conservation of mass and momentum which we take in Eulerian form, namely,

$$\frac{\partial\rho}{\partial t}+u\frac{\partial\rho}{\partial x}+\rho\frac{\partial u}{\partial x}=0 \quad \text{(B3)}$$

and

$$\frac{\partial u}{\partial t}+u\frac{\partial u}{\partial x}+\frac{dP}{d\rho}\frac{\partial\rho}{\partial x}=0. \quad \text{(B4)}$$

Let

$$\omega = \int_{\rho_1}^{\rho} c\frac{d\rho}{\rho} = \int_{\rho_1}^{\rho}\left(\frac{dP}{d\rho}\right)^{\frac{1}{2}}\frac{d\rho}{\rho} = \frac{2c_1}{\gamma-1}\left[\left(\frac{\rho}{\rho_1}\right)^{(\gamma-1)/2}-1\right] = \frac{2c_1}{\gamma-1}\left[\left(\frac{P}{P_1}\right)^{(\gamma-1)2/\gamma}-1\right], \quad \text{(B5)}$$

where the last two expressions hold in virtue of the perfect gas assumption which leads to (B1). We rewrite Eqs. (B3) and (B4) in terms of ω and u and after multiplying (B3) by c/ρ, obtain:

$$\frac{\partial\omega}{\partial t}+u\frac{\partial\omega}{\partial x}+c\frac{\partial\omega}{\partial x}=0$$

$$\frac{\partial u}{\partial t}+u\frac{\partial u}{\partial x}+c\frac{\partial\omega}{\partial x}=0.$$

Adding and subtracting we then find

$$\frac{\partial r}{\partial t}+(c+u)\frac{\partial r}{\partial x}=0$$
$$\frac{\partial s}{\partial t}-(c-u)\frac{\partial s}{\partial x}=0 \quad \text{(B6)}$$

where

$$r=\tfrac{1}{2}(\omega+u), \quad s=\tfrac{1}{2}(\omega-u).$$

These equations state that constant values of r and s are propagated with velocities $u+c$ and $-(c-u)$, respectively. For a disturbance traveling in only one direction we have either r or s constant. By the introduction of the lower limit of integration we have insured that $\omega_1=0$ and hence $u-u_1=\pm\omega$. This equation together with (B5) enables us to determine the expressions analogous to those derived in Appendix A.

In case $s=$ constant we may solve the remaining equation of (B6) by the following procedure. If $r=$ constant a similar discussion can be made. The first of Eqs. (B6) becomes

$$\frac{\partial\omega}{\partial t}+\Gamma(\omega)\frac{\partial\omega}{\partial x}=0, \quad \text{(B7)}$$

where

$$\Gamma(\omega)=c(\omega)+\omega$$

and $c(\omega)$ is the function obtained from solving (B5) for ρ/ρ_1 as a function of ω and substituting this in the expression for c as a function of ρ/ρ_1, namely,

$$c=\left(\frac{dP}{d\rho}\right)^{\frac{1}{2}}=\frac{\gamma P_1}{\rho_1}\left(\frac{\rho}{\rho_1}\right)^{(\gamma-1)/2}=(\gamma-1)\omega/2+c_1.$$

Thus

$$\Gamma(\omega)=(\gamma+1)\omega/2+c_1.$$

The general solution of (B7) is

$$f(\omega)=x-\Gamma(\omega)t, \quad \text{(B8)}$$

where $f(\omega)$ is an arbitrary function of ω. For any specific problem it must be determined from the boundary conditions describing the disturbance.

APPENDIX C. DENSITY FIELD IN MACH REFLECTION

At the time this paper was submitted (November 1948) no data were available on the detailed density field associated with the Mach reflection of a shock wave although some interferometric measurements had been made on shock intersections in wind tunnels and jets.[16] Recent new results makes it advisable to bring the subject up to date by the addition of this appendix as the manuscript goes to press (July 1949).

In the shock tube now in use at Princeton the density field[26] associated with the reflection phenomenon

[26] Bleakney, Weimer, and Fletcher, Phys. Rev. 75, 1294A (1949).

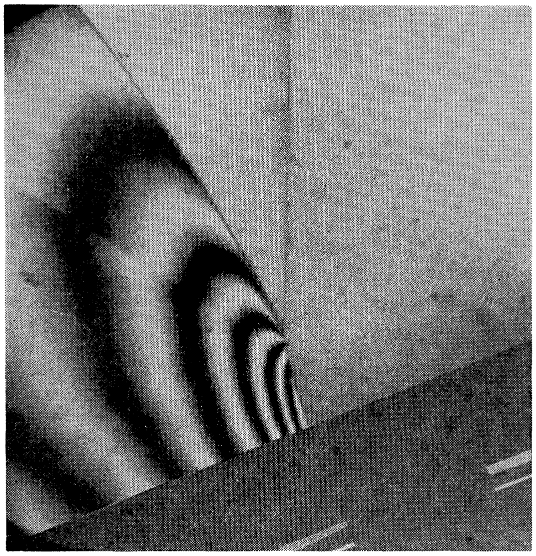

FIG. 17. Interferogram of Mach reflection ($\alpha=68.2°$, $\xi=0.88$). The fringes represent density contours or isopycnic lines in the gas.

has been examined with an interferometer. A flash photograph, reproduced in Fig. 17, is made with the "single fringe" adjustment of the instrument, i.e., constant difference in light path over the entire field of view in the absence of any disturbance. The fringes that appear as a result of the reflection process are contours of constant fringe shift and hence contours of constant density in the gas. The parameters α and ξ have the values 68.2° and 0.88, respectively. The angle χ in this case is 1.5°. The weak shock following the reflected wave looks suspicious but investigation has shown that it arises from some extraneous disturbance having no relation to the reflection phenomenon. For such weak incident shocks the density jump across the slip stream is too small to be evident.

If the fringe number is taken to be 0 in the undisturbed region ahead of the incident shock in Fig. 17 then, to the nearest fringe, the number is 6 between the incident and reflected shock and 16 for the first white fringe behind the Mach shock near the wall. As one proceeds down the inclined wall the numbers decrease in order.

There are several points of interest in these new results. The density and pressure are uniform in the angular region between the incident and reflected wave to a high degree. Behind the Mach branch and near the wall the density falls (gradρ points forward toward the shock). Behind the reflected wave and near the triple point the density rises to a maximum and falls again (gradρ points away from the shock but reverses as the point of observation moves toward the corner). Near the triple point the density behind the reflected wave varies strongly with angle and very little with radius from this point. The variation does not seem to be truly angular however since all of the contours do not converge toward the triple point.

Since the characteristics of the density pattern in Fig. 17 resemble those in the solution of Bargmann[24] for the case of nearly glancing incidence, it becomes especially interesting to examine experimental results for an angle of incidence as close to this case as possible. In his paper Bargmann shows that for weak shocks ($\xi \geqq 0.8$) and nearly glancing incidence the density jump across the slip stream, the vorticity behind the curved reflected wave and the anisentropy in this region are negligible. Under these conditions he solved the hydrodynamical problem of Mach reflection for the positions and strengths of the shocks, the density pattern and the flow velocities in terms of $e=\tan(\pi/2-\alpha)$ when this quantity is small. It turns out that in first approximation in e the reflected wave R is not a shock at all, that is, the pressure varies continuously across it but there is a discontinuity in the pressure gradient at R. In second approximation the pressure is discontinuous at R so that the strength of this shock is of order e^2. However in this approximation the strength of the reflected shock still goes to zero as the triple point is approached. This means that a maximum must exist at some point along its length.

Figure 18 is a "single fringe" adjusted interferogram of a Mach reflection with $\alpha=80°$ and $\xi=0.8$. The numbers on this figure refer to calculated fringe shifts and the accuracy is of the order of ± 0.5 fringe. The curves drawn in the figure represent the position of the shock waves and the density contours computed by the method given in Bargmann's paper.

It will be noticed that the theoretical positions of the shocks and the observed ones agree almost perfectly in the vicinity of the triple point and above this point. However, the observed and theoretical positions of the Mach shock are not quite the same near the wall.

There is some disagreement between the computed density contours and the lines of constant fringe shift. As has been remarked, the latter may be somewhat in error. Bargmann's results agree better with experiments on weaker shocks being reflected at more glancing angles as is to be expected from the approximations and boundary conditions he uses. However for the conditions under which Fig. 18 was obtained there is still qualitative agreement between the shape of the fringe pattern and the computed density contours in the vicinity of the reflected shock. Near the wall the disagreement is more pronounced. This is probably due to the fact that the boundary conditions used by Bargmann in his weak shock and glancing incidence theory are not applied at the wall itself but at a horizontal line through the corner of the wall. Thus one would expect the difference between theory and experiment to be more noticeable near the wall. The fact that the Mach wave is observed ahead of its predicted position is consistent with the higher than predicted density just behind it.

APPENDIX D. LIST OF SYMBOLS

		Page
u, u^i	Velocity and velocity components of a gas or piston	584
c	Velocity of sound	584
ξ^i	Lagrange coordinates	584
x^i	Euler coordinates	584
d/dt	Partial differentiation with respect to t for fixed x^i	585
$\partial/\partial t$	Partial differentiation with respect to t for fixed x^i	585
$V(t)$, V_0, $V_1(t)$, $V_2(t)$	Volumes occupied by a fluid at time t	585
$S(t)$, S_0, $S_1(t)$, $S_2(t)$	Surfaces bounding volumes $V(t)$	585
λi	Direction cosines of the normal to a surface	585
$[f]$	The discontinuity in a function f	585
m	Rate of matter crossing unit area of a discontinuity	585
V^i, V_n, V	Velocity components of a discontinuity	585
P, P_1, P_2	Pressures	586
ρ	Density	586
U	Internal energy per unit mass	586
T	Temperature	586
	Also used to denote triple point	594
S	Entropy per unit mass	586
α	Angle of incidence	586
γ	Ratio of specific heats of a gas	590
y	Ratio of pressure behind a shock to that in front	590
$\xi=1/y$	Ratio of pressure in front of a shock to that behind	590
α_s	Sonic angle of incidence	593
χ	Angle the line of travel of the triple point makes with the wall	594
α_0	Angle of incidence for which $\chi=0$	595
ω	Angle between flow and incident shock (Fig. 12)	595
ω'	Angle between reflected shock and path of the triple point (Fig. 12)	595
Z, Z', Z_1	Velocity of flow vectors (Fig. 14)	596
τ, τ'	Angles between flow vectors and normals to shocks (Fig. 14)	597
δ, δ'	Angles of deflection of a flow by a shock (Fig. 14)	597
$\eta=\rho'/\rho$	Compression ratio, ratio of density behind a shock to that in front of it	597
α_e	Extreme angle, angle of incidence for which regular reflection is no longer theoretically possible	599

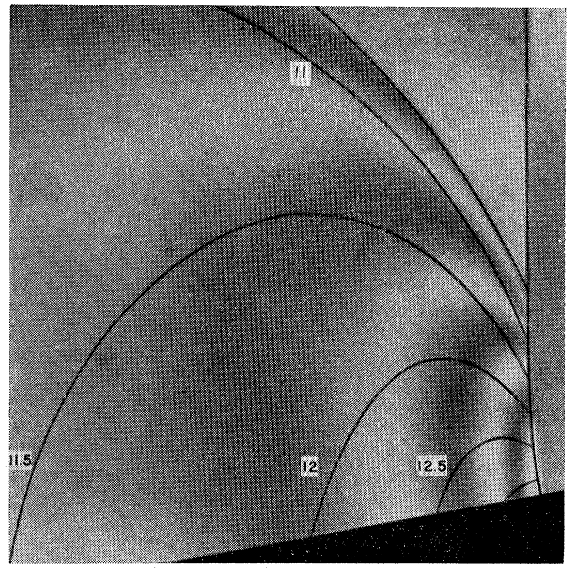

FIG. 18. Isopycnic interferogram of Mach reflection ($\alpha=80°$, $\xi=0.8$). The curves superposed on the photograph represent the calculated positions of the shock waves and the density contours.

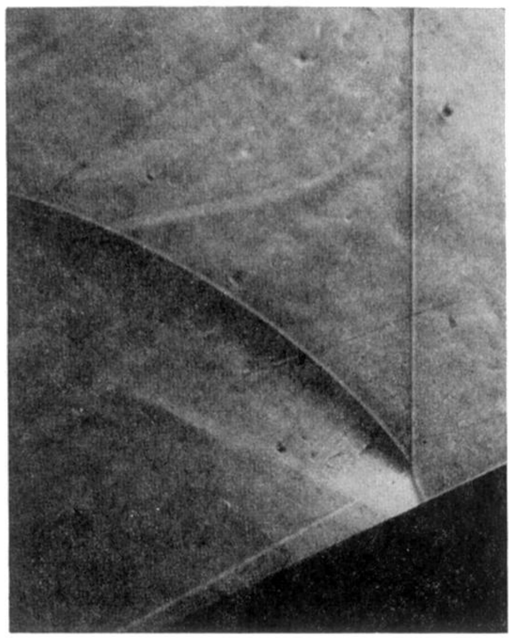

FIG. 10. A photograph of Mach reflection taken by the schlieren method.

FIG. 17. Interferogram of Mach reflection ($\alpha = 68.2°$, $\xi = 0.88$). The fringes represent density contours or isopycnic lines in the gas.

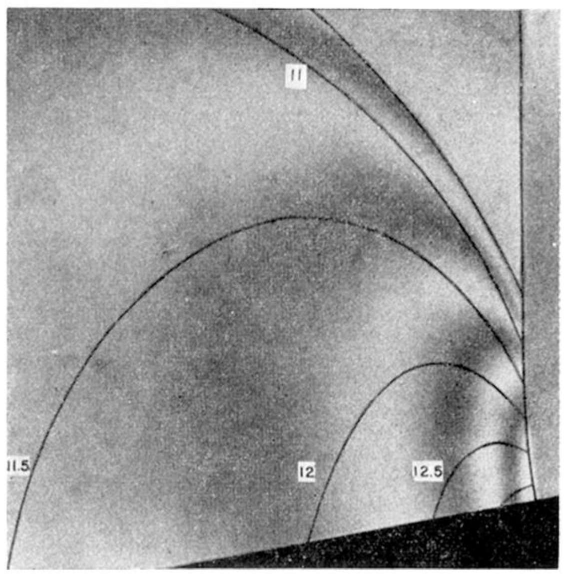

FIG. 18. Isopycnic interferogram of Mach reflection ($\alpha=80°$, $\xi=0.8$). The curves superposed on the photograph represent the calculated positions of the shock waves and the density contours.

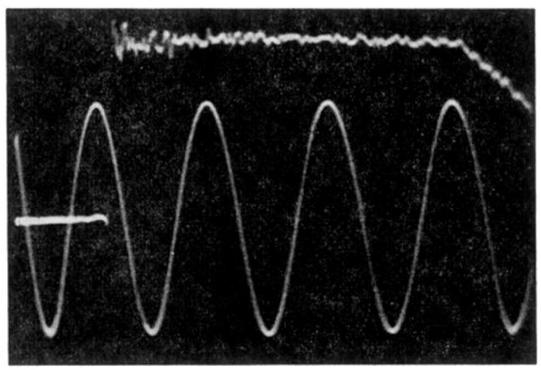

FIG. 4. A quartz gauge pressure-time oscillogram of a shock wave in the tube. The vertical displacement represents pressure. Also shown is a 1000-cycle sine-wave which determines the horizontal time scale.

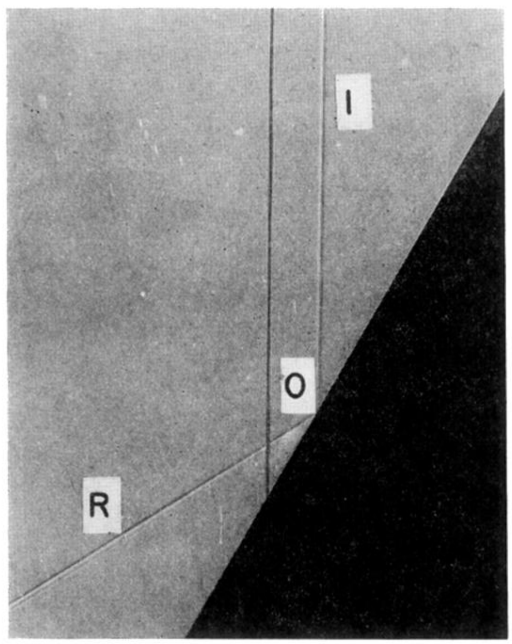

FIG. 7. A shadow picture of a regular reflection. The incident wave I is vertical and traveling to the right it makes an angle of 29° with the barrier which is represented in the figure by the solid black portion. The reflected wave R makes an angle of 27° with this barrier. The solid black line is a plumb line used for reference.

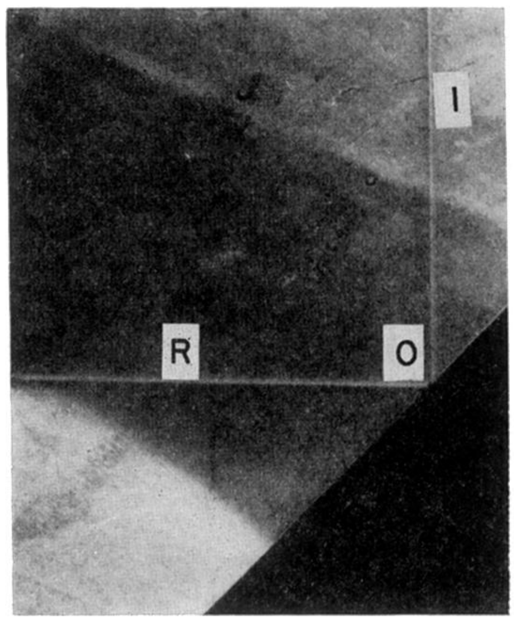

FIG. 8. A schlieren photograph of regular reflection. I and R are the incident and reflected shocks. The sound wave from the corner can be seen in the lower left-hand portion of the figure.

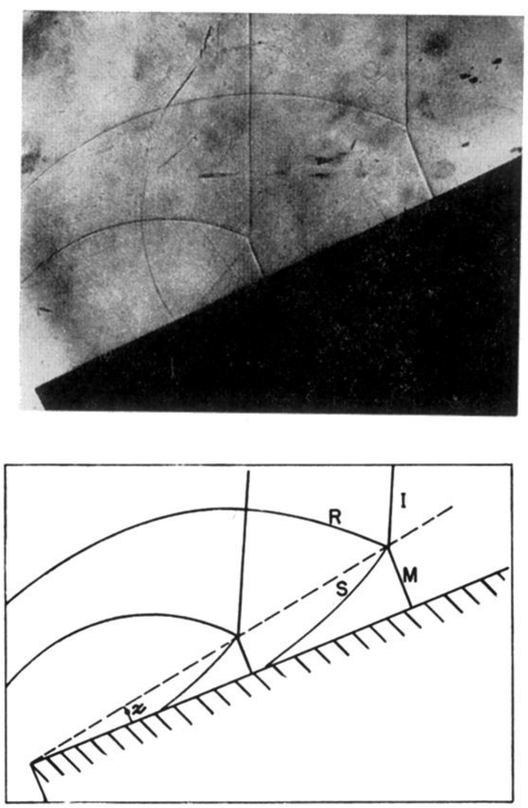

a

b

FIG. 9. A double exposure of Mach reflection by parallel shadow. 9a is the original and 9b is a tracing of the discontinuities. I, R, and M represent the incident, reflected, and Mach shocks and S represents the slip stream.